

Author's Response

Contents

1. Response to referee#1 (RC#1)
2. Response to referee#2 (RC#2)
3. Response to short comment#1 (SC#1)
4. Marked-up manuscript
5. Marked-up supplementary file

Response to referee#1 (RC#1)

Response to the anonymous reviewer comments (RC1)

Interactive comment on “Mixed layer depth variability in the Red Sea” by Cheriyei P. Abdulla et al.

Referee #1

Received and published: 29 March 2018

General Comments:

The authors have used historical temperature profiles from the Red Sea to develop a monthly climatology of mixed layer depth (MLD) along the seas' central axis, and investigate the importance of wind stress, thermal buoyancy forcing and haline buoyancy forcing in controlling MLD in the northern, central and southern Red Sea. The authors also investigate the relationship between MLD and the presence of cyclonic and anticyclonic mesoscale eddies, as well as the impact of the cross-axis Tokar Gap wind jet on MLD in summer.

To my knowledge, this is the first published climatology of MLD in the Red Sea, which will be useful for verifying numerical model simulations of the basin and biogeochemical studies. The analysis of the impact of atmospheric forcing mechanisms as a function of latitude is interesting and worth publishing, in my view. The descriptions of the impacts of mesoscale eddies and the Tokar Gap wind jet are less clear and I recommend major revisions in these sections to make them truly convincing.

Answer:

We thank the reviewer for his valuable comments and suggestions. The comments and suggestion were very helpful in improving the manuscript. Necessary improvements are done in the sections explaining the effect of eddies and Tokar gap jet winds. The direct effect of wind apart from the effect of wind induced secondary circulation (the cyclonic and anticyclonic eddies) was not clear in the earlier version of the manuscript, which is solved in the new version of manuscript. The answers to both specific and technical comments are given below, and required modifications are made in the manuscript.

Please note that coloured text is used in few instances of this document to represent modified/deleted text.

Red: the modified/deleted text in the earlier version of the manuscript

Blue: the modified text in the new version of the manuscript.

Specific Comments:

Specific Comment-1:

Line 30 – Much of this is elementary physical oceanography, belonging in a textbook, not a scientific paper. I suggest to condense this part of the text significantly.

Answer:

We agree with the reviewer in this, our intension was to refresh the memories of the readers with the effect of each parameters on the mixed layer depth. As suggested by the reviewer, the paragraph is shortened as follows. In this, we show the two paragraphs before and after modification.

Earlier version of the paragraph

Surface mixed layer is a striking and universal feature of the open ocean where the turbulence associated with various physical processes leads to the formation of a quasi-homogeneous layer with nearly uniform properties. The thickness of this layer, often named mixed layer depth (MLD), is one of the most important oceanographic parameters, as this layer directly communicates and exchanges energy with the atmosphere and therefore has a strong impact on the distribution of heat (Chen, Busalacchi, & Rothstein, 1994), ocean biology (Polovina, Mitchum, & Evans, 1995) and near-surface acoustic propagation (Sutton, Worcester, Masters, Cornuelle, & Lynch, 2014). Heat and fresh-water exchanges at the air-sea interface and wind stress are the primary forces behind turbulent mixing. Similarly, stirring associated with turbulent eddies predominantly changes the mixing process, mainly along the isopycnal surfaces where stirring may occur with minimum energy (de Boyer Montégut, Madec, Fischer, Lazar, & Iudicone, 2004; Hausmann, McGillicuddy, & Marshall, 2017; Kara, Rochford, & Hurlburt, 2003).

Oceanic heat loss cools the mixed layer and weakens the stratification, leading to strong mixing and a deeper MLD. Similarly, the heat gain warms the mixed layer and strengthens the stratification, leading to weak mixing and shallow MLDs. The fresh-water loss makes the surface water more saline and denser, leading to enhanced mixing and deeper MLDs, while the fresh-water gain makes the surface water fresher and lighter, leading to diminished mixing and shallow MLDs. The momentum transmitted to the ocean through from the wind stress acts as the primary dynamic force for the upper layer turbulence and circulation. The shear and stirring generated by the wind stress enhance the vertical mixing and play a major role in controlling the deepening of the oceanic mixed layer. In some regions, the mixed layer variability is mainly controlled by wind stress.

New version of the paragraph (modified text in blue colour)

The surface mixed layer is a striking and universal feature of the open ocean where the turbulence associated with various physical processes leads to the formation of a quasi-homogeneous layer with nearly uniform properties. The thickness of this layer, often named mixed layer depth (MLD), is one of the most important oceanographic parameters, as this layer directly communicates and exchanges energy with the atmosphere and therefore has a strong impact on the distribution of heat (Chen et al., 1994), ocean biology (Polovina et al., 1995) and near-surface acoustic propagation (Sutton et al., 2014). Heat and fresh-water exchanges at the air-sea interface and wind stress are the primary forces behind turbulent mixing. The loss of heat and/or freshwater from the ocean surface can weaken the stratification and enhance the mixing and vice versa. The shear and stirring generated by the wind stress enhance the vertical mixing and play a major role in controlling the deepening of the oceanic mixed layer. Further, the stirring associated with turbulent eddies predominantly changes the mixing process, mainly along the isopycnal surfaces where stirring may occur with minimum energy (de Boyer Montégut et al., 2004; Hausmann et al., 2017; Kara et al., 2003).

[Lines: 20-33]

Specific Comment-2:

Line 43 – Bower and Farrar (2015) have direct estimates of evaporation rates that should be mentioned and referenced here.

Answer:

The suggested reference of Bower and Farrar (2015) is appropriate to the context and added to the manuscript.

[Lines: 56]

Specific Comment-3:

Line 148 and following – 85 m ± what? Need to add standard deviations to these mean values, in this line and all the following instances of reporting mean values. This is essential to understanding the statistical significance of the mean values. I realize some statistics are included in the supplementary material, but they should be included in the main document. Similar for lines 152–153, line 175 and line 197 (plotted lines need error bars or similar).

Answer:

The range of observed MLD values and the standard deviation from mean value are included at appropriate instances. The text is modified accordingly. The error-bars are added to the figure describing the monthly climatology of NHF, evaporation and precipitation, and wind stress (Figure 5).

The figure 4 shows monthly values from a single year (2016), with one value for each month. Therefore, we have not included the error bars.

Modified text

A Hovmoller diagram of the monthly MLD climatology is presented in Fig. 3. The deepest MLD is observed in February and the shallowest during May-Jun. A significant annual variability is observed in the Red Sea. The maximum value of climatological mean MLD is observed in February at the northern Red Sea while the minimum noticed at various instances, especially during summer months. The MLD of individual profiles in the northern Red Sea has a wide range of values from 40 to 120 m mainly due to the presence of active convection process, while some of the profiles show MLD deeper than 150 m in consistence with Yao et al., (2014). Apart from the northern deep convection region, the south-central Red Sea between 18 °N-21 °N (53±5 m) and 14 °N-16 °N (48±9 m) also experienced deeper MLDs during the winter, which is separated by a shallower MLD around 17 °N (44±14 m). During

July to September, the region around 19 °N experienced a deeper mixed layer in contrast with the general pattern of summer shoaling over the entire Red Sea.

[Lines: 190-202]

Specific Comment-4:

Line 214 – It wasn't obvious to this reviewer how the authors chose the latitudes where there were supposedly reductions in correlation between MLD and all forcing mechanisms. For some of the gray bars, the coincidence of lower correlations is obvious, but not in all. Would be good to define more clearly how these latitudes were chosen, hopefully using some objective criteria.

Answer:

As pointed out by the reviewer, we have selected the latitude bands (13.5 °N, 17.5 °N, 19 °N, 23 °N, and 26.5 °N) based on the observed drop in correlation for all the forces. We agree that there is a small difference in the case of 23 °N. At this latitude, the heat flux and wind stress have a clear coinciding drop in correlation while correlation for freshwater has a small increase. But, considering the correlation values for freshwater from 22 °N and 24 °N, the correlation is dropped around 23 °N (between 22 °N and 24 °N), even though a small local increase is seen at 23 °N. Therefore, we considered 23 °N as the region of coinciding drops in correlation.

[Lines:297]

Specific Comment-5:

Line 243 – References are needed here to validate the authors' description of the relationship between mesoscale eddies and MLD.

Answer:

Appropriate references were added to the text (Dewar, 1986; Fox-Kemper, Ferrari, & Hallberg, 2008; Hausmann et al., 2017; Smith & Marshall, 2009; de Boyer Montégut et al., 2004; Chelton et al., 2004, 2011).

[Lines: 332-339]

Specific Comment-6:

Line 267 - The authors are implicitly arguing that the upwelling and downwelling associated with the secondary circulation of cyclonic and anticyclonic eddies is more important in determining MLD in the eddies than direct wind forcing and buoyancy forcing. Is there any literature to support this? I'm guessing there is, and the authors need to add some references here to this point.

Answer:

As mentioned in the reply to comment #5, appropriate references discussing the importance and dominance of eddy effect on MLD variability are added to the manuscript. The results from the literature (de Boyer Montégut et al., 2004; Chelton et al., 2004, 2011; Dewar, 1986; Fox-Kemper et al., 2008; Hausmann et al., 2017; Smith & Marshall, 2009) have shown that eddies can efficiently re-stratify the ocean, dominating over the existing effect of wind stress and net heat flux over the region. The studies also show that the resultant effect of eddy is largely dependent on the eddy amplitude, and the mixing intensity is largest at the centre of eddy.

[Lines: 338-339]

Specific Comment-7:

Line 322 - It is not clear to me here if the region to the south of the jet axis is well-mixed because of wind-induced turbulent mixing, or because of the secondary circulation associated with the wind stress curl-

induced formation of the anticyclonic eddy, or both. the authors need to clarify this, or, if it is ambiguous, say that they are not sure which mechanism dominates.

Answer:

It is true that the wind-induced turbulent mixing obviously exists on both side of the Tokar jet axis. The secondary circulation formed by the Tokar winds, with different polarities on both side, cyclonic to the north of the Tokar-axis and anticyclonic to the south, acts in opposite direction to the vertical mixing. The mixing in the Tokar region is the sum of both the wind-induced turbulent mixing and the secondary circulation (eddies). A proper quantification of the contribution each mechanism needs further investigations.

[Lines: 438-449]

Specific Comment-8:

Line 326 - If this is a summary sentence, I suggest to start it with “In summary. . .”

Answer:

The text is changed accordingly.

[Lines: 442]

I'm left with uncertainty about the authors' claim regarding the role of the TG jet in increasing MLD. As questioned above, does the upwelling and downwelling associated with the eddies overwhelm the direct mixing impact of the wind jet? Presumably the direct impact of the winds would be felt on both sides of the wind jet axis, but it's not clear if the authors are making this point for the cyclonic as well as anticyclonic eddy. Clarification needed here.

Answer:

As mentioned in the reply to comment #7, we agree that the turbulence is present on both sides and enhances mixing. But eddy effect is in opposite directions in the northern and southern sides of Tokar-axis, and therefore the signature is evident in the mixed layer depth structure, with enhancement of mixing in the southern side and reducing the mixing in the northern side (please refer to Figures 10 and 11).

[Lines: 414, 425, 438-445]

Specific Comment-9:

Line 346 – It was not clear to me if the deeper MLD was due to the direct impact of the winds or the formation of the anticyclonic eddy. Needs clarification.

Answer:

As mentioned in the reply to comment #7 and #8, the contribution of both the wind and secondary circulation are simultaneously existed in the Tokar region. In the earlier version of the manuscript, the contribution of direct wind turbulence was not clearly mentioned in the conclusion part. In the revised version of the manuscript, we corrected the text and clearly stated that the mixing in the region is a combination effect of both wind turbulence and eddies.

[Lines: 464-481]

Specific Comment-10:

Line 350 - I think this is the best result of the paper.

Answer:

We thank the reviewer for appreciating this part of the result.

Specific Comment-11:

Line 357 - As remarked on above, why would the winds enhance ML development south of the wind axis but not north? Maybe the deepening to the south is due mostly/only to the formation of the anticyclonic eddy?

Answer:

As stated in replies to comments#7 to 9, the wind enhance mixing on both side of the Tokar-axis. The text also corrected accordingly.

The deepening in the south of Tokar axis is the combined effect of both wind and anticyclonic eddy, while shoaling in north is due to the opposite (diminishing) effect of the cyclonic eddy.

[Lines: 491-493]

Technical comments:

Technical comment-1:

Line 20 – Should read “The surface mixed layer . . .” (i.e., add “the”)

Answer:

The manuscript is corrected as suggested.

[Lines: 20]

Technical comment-2 to 4:

Line 30 – Should read “Oceanic heat loss. . .” (i.e., delete “The”)

Line 30 – “to strong mixing. . .” “Strong”? Compared to what?

Line 35 – “through from. . . .” Extra word here.

Answer to Technical comment-2 to 4:

The manuscript is corrected accordingly. This paragraph is modified and summarised.

[Lines: 27-30]

Technical comment-5:

Line 39 – “The Red Sea is a typical. . . .” How is it typical?

Answer:

The text is corrected and removed the usage “typical”.

We have used this word considering that the Red Sea is a typical inverse estuarine system, where the evaporation is dominated over the precipitation.

[Lines: 34]

Technical comment-6:

Line 45 – “regions in the world. . .” Referring to the water in the Red Sea? Maybe use “ocean basin” instead of “region.”

Answer:

The manuscript is corrected as suggested.

[Lines: 40]

Technical comment-7:

Line 48 – What about Yao et al. references? Shouldn't they be included here? They represent some of the most comprehensive modeling studies of the Red Sea to date (after Sofianos' papers).

Answer:

The manuscript is corrected as suggested and the references are added.

[Lines:42-43]

Technical comment-8:

Line 49 – The increase in the number of temperature. . .” (add “the number of”)

Answer:

The manuscript is corrected as suggested.

[Lines: 44]

Technical comment-9:

Line 55 – the authors should consider adding reference to Bower and Farrar (2015) paper and Yao et al. papers.

Answer:

The manuscript is corrected as suggested and the references *are added*.

[Lines: 49-50]

Technical comment-10:

Line 77 – Over what depth range are inversions flagged?

Answer:

Over upper 500 meters, which could be sufficient for the MLD estimation in the Red Sea.

Technical comment-11:

Line 89 – What does “spread” mean? I think the word to be used is “distribution.”

Answer:

The text corrected as suggested.

[Lines: 83]

Technical comment-12:

Line 110 – “Traon” Check spelling. I think it’s “LaTraon”.

Answer:

The text corrected as suggested.

[Lines: 113]

Technical comment-13:

Line 118 – What is meant by short-range disturbances? A sentence or two more on how the method works will save the reader from having to look it up elsewhere.

Line 121 – Would be helpful to the reader to give an example. How exactly does this work?

Answer:

A brief description on the estimation of MLD using “segment method” is added in the manuscript, with the help of a sample profile.

The text added in the manuscript:

The MLD can be estimated based on different methods. The Fig.2 shows a sample temperature profile collected on 19th January 2015 from Red Sea (24.9° N, 35.18 °E), with short-range gradients within the mixed layer. This gradient could rise from instrumental errors or turbulence in the upper layer. The curvature method (Lorbacher et al., 2006) identified MLD at 32 m, due to the presence of a short range gradient at this depth. Threshold method (de Boyer Montégut et al., 2004) detected MLD at 130 m (threshold = 0.2 °C), while segment method identified MLD at 120 m. The segment method based MLD could be considered as a reliable estimate comparing to both curvature (under estimation) and threshold method (over estimation). The segment method first identifies the portion of the profile with significant inhomogeneity where the transition from a homogeneous layer to inhomogeneous layer occurs. Then, this portion of the profile is analyzed to determine the MLD (detailed procedure of the estimation technique is given Abdulla et al., 2016). In the present study, MLD is estimated based on the segment method, which is found to be less sensitive to short-range disturbances within the mixed layer (Abdulla et al., 2016). This method first identifies the portion of the profile (segment) where the transition from a homogeneous layer to inhomogeneous layer occurs. Then, this segment is analyzed to determine the MLD.

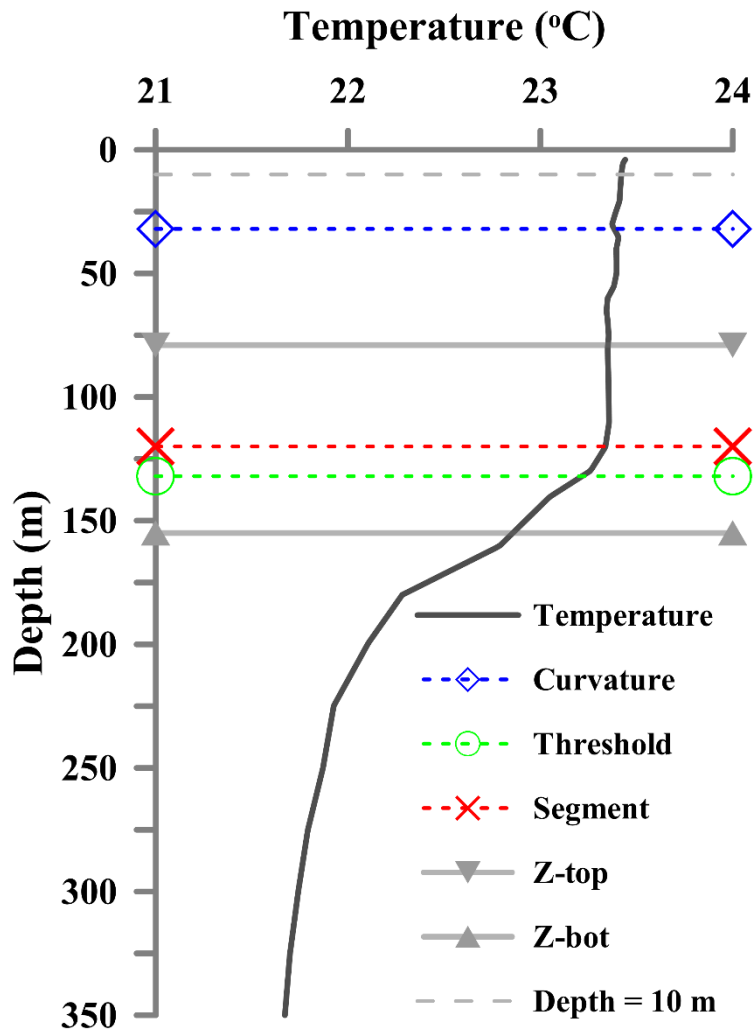


Figure. The MLD estimated for a schematic temperature profile based on curvature, threshold, and segment methods. Z-top and Z-bot represents the top and bottom ends of the portion of the profile with significant inhomogeneity.

[Lines: 119-161]

Technical comment-14:

Line 149 – Are these numbers from individual profiles? Please clarify.

Answer:

Yes, these numbers are from individual profiles. The same is mentioned in the text also.

The text from the manuscript

The MLD of individual profiles in the northern Red Sea has a wide range of values from 40 to 120 m mainly due to the presence of active convection process, while some of the profiles show MLD deeper than 150 m in consistence with Yao et al., (2014).

[Lines: 191-193]

Technical comment-15:

Line 158 – This sentence is confusing. What is meant by the “other regions”?

Answer:

The sentence is corrected. “other regions” is replaced with “other parts of the Red Sea”

The text from the manuscript

Compared to other parts of the Red Sea, during November and December, relatively shallower MLDs were witnessed at approximately 16 °N-17 °N, and 24.5 °N-26.5 °N.

[Lines: 218-220]

Technical comment-16:

Line 168 – I would say April to June is more like the monsoon transition (probably low winds), not summer.

Answer:

The text is corrected accordingly.

[Lines: 229-230]

Technical comment-17:

Line 174 – “net heat loss” (loss not lose)

Answer:

The text is corrected accordingly.

[Lines: 236]

Technical comment-18:

Line 180–181 – Rather than “enhance mixing,” which should be “enhances mixing” to be grammatically correct, I would suggest saying “supports vertical mixing through buoyancy loss” or something similar.

Answer:

The text is corrected accordingly

[Lines: 242-243]

Technical comment-19:

Line 181 – “slightly diminishes mixing. . .” And here I would say “opposes vertical mixing due to buoyancy gain.”

Answer:

The text is corrected accordingly

[Lines: 243-244]

Technical comment-20:

Line 184 – Would be helpful to define acronyms in figure caption.

Answer:

The figure caption is corrected accordingly

The changes caption from the manuscript

Figure 3. Time series of heat flux components (incoming shortwave radiation (SWR), long wave radiation (LWR), latent heat flux (LHF), sensible heat flux (SHF) and net heat flux (NHF)) for the year 2016 in the central Red Sea.

[Lines: 251-253]

Technical comment-21:

Line 190 – “support vertical mixing” (add “vertical”)

Answer:

The text is corrected as suggested.

[Lines: 204]

Technical comment-22:

Line 192 – Shouldn't it be “net buoyancy flux” ?

Answer:

The text corrected accordingly.

[Lines: 259]

Technical comment-23:

Line 194 – Isn't there a Sofianos paper to be referenced here too? Figures 3 and 4 – It would be helpful to add a zero Line on Figs. 3 and 4.

Answer:

The reference of *Sofianos paper* is included accordingly.

[Lines: 264-265]

The zero lines are inserted in the figure 3 and 4

[Lines: 250, 266]

Technical comment-24:

Line 200 – I suggest that the authors mention the wind direction as well as stress amplitude variations through the seasons. Also, shouldn't wind stress in the winter be negative? All wind stress values are presented as positive. This is okay since it is only the magnitude (not direction) that impacts vertical mixing, but the authors need to say they are showing absolute value only.

Answer:

The Figure in the earlier version of manuscript show the “magnitude of wind stress” alone. As mentioned by the reviewer, the East and North components of wind stress along with absolute wind stress are presented in the figure 5.

[Lines:266]

Technical comment-25:

Line 206 – I'm not sure what the authors mean here by “phase.” I think they are referring to negative and positive correlation; e.g., MLD and NHF are negatively correlated since as NHF (into the ocean) increases, MLD decreases.

Answer:

The text is corrected accordingly as follows.

The wind stress and E-P are positively correlated with MLD while the NHF is negatively correlated since as NHF (into the ocean) increases, MLD decreases. For simplicity of the figure (Figure 5), the correlation values of all parameters are presented as positive.

[Lines: 279-282]

Technical comment-26:

Line 229 - How were eddies identified? If some eddies or sub-gyres are semi-permanent, how do you decide when one 'dies' and a new one is formed? If the histogram is from another paper, it should be referenced here.

Answer:

Eddies are identified based on “winding angle” method. The identification is done by Zhan et al., 2014. The reference is mentioned in the text as well as in the caption of the histogram (Fig. 7).

[Lines: 308-309 and 335]

Technical comment-27:

Line 258 - I think 'curve' should be 'curves,' because the point is (I think) that at these latitudes, correlations between MLD and all the forcing factors (wind, thermal buoyancy, haline buoyancy) are reduced.

Answer:

The text is corrected accordingly

[Lines: 362]

Technical comment-28:

Line 260 - Zhai and Bower 2013 should be added to this list, and Bower and Farrar 2015.

Answer:

These references are added to the list.

[Lines: 364]

Technical comment-29:

Line 289 – Authors should indicate data source in figure caption.

Answer:

The wind data is CFSR hourly wind product. The same mentioned in the caption also.

[Lines: 394]

Technical comment-30:

Line 291 – What is the data source for the T S profiles?

Answer:

The temperature and salinity profiles are from Sofianos and Johns, 2007, and the same is mentioned in the figure caption.

Caption

Figure 9. (a) The CTD measured temperature and salinity profiles during 13-14 Aug 2001. (b) SLA maps and (c) wind speed and direction (averaged for the previous one week) in the Tokar region, before, during and after the Tokar event. The temperature and salinity profiles are received through personal communication from (Sofianos & Johns, 2007).

[Lines: 412-416]

Technical comment-31:

Line 293 - This year (2001) was also highlighted and described by Zhai and Bower 2013, which should be referenced here.

Answer:

The suggested reference is added in the manuscript.

Text from the manuscript

The temperature and salinity profiles measured during summer 2001 (13-14 Aug 2001), which coincided with the Tokar event are shown in Fig. 9a-b (Sofianos and Johns, 2007; Zhai and Bower, 2013).

[Lines: 397-398]

Technical comment-32:

Line 333 - “slightly lower” than what? Lower than some individual measurements? If that is what is meant, that is obvious and this phrase should be deleted, or replaced with the actual extreme values.

Answer:

The text is corrected accordingly.

[Lines:453]

Technical comment-33:

Line 334 - Rather than ‘general picture’, authors should say something more concrete like ‘climatological mean.’

Answer:

The text is corrected accordingly.

[Lines: 454]

Technical comment-34:

Line 340 - I would say that shallow MLD and increased stratification are the same thing. Authors could consider ‘associated with increased short-wave radiation’ instead.

Answer:

The text is corrected accordingly.

[Lines: 459-460]

Technical comment-35:

Line 343 - Suggest to add "...is not linear with increasing latitude."

Answer:

The text is corrected accordingly.

[Lines: 475]

Technical comment-36:

Line 345 - This phrase is confusing. Suggest to say "deeper MLD than typical of elsewhere in the Red Sea" or something similar.

Answer:

The text is corrected accordingly.

[Lines: 478]

Answer to reviewer comments-Supporting information

SI-Comment-1:

Figure S1 – I think “distribution” is a better word than “spread.”

Answer:

The text is corrected accordingly.

[Lines: 27 and 45]

SI-Comment-2:

Table S1 – I don’t think it’s necessary to include this table. It was sufficient to describe the end result of the QC in the manuscript.

Answer:

This Table is removed. The manuscript is modified accordingly.

SI-Comment-3 and 4:

Table S2 – Could this information be summarized more efficiently with a plot of some kind?

Table S3 – Similar comment for this table. Change to a plot?

Answer:

As suggested by the reviewer, the tables S2, S3 and S4 are converted into plots.

[Lines: 52, 61, and 70]

Response to referee#2 (RC#2)

Interactive comment on “Mixed layer depth variability in the Red Sea” by Cheriyeri P. Abdulla et al.

Referee #2

Received and published: 1 May 2018

General comments:

The paper is generally well-executed and well-written, although it does need some editing. The authors say that MLD results are not available from previous research, but I am not competent to judge that, so I will take them at their word on that point.

There is a lot of good material here, but I also have reservations about some of it. These comments are summarized below. Please note that these comments are not in order of importance, but are in the order I encountered the material in the paper.

The bottom line is that the basic description is well-done and should be published.

The special latitude bands identified in the correlation plot are not proven to be real, at least to my satisfaction, but the Tokar Gap signal at 19N is interesting and corresponds to a clear “tongue” in the MLD climatology.

I’m ignoring a rule I agree with that we cannot just point to features in a plot and interpret these without a “null” test that the feature could be noise, but we’ll discuss that more down below.

The paper would be much better if you were to get rid of the AVISO SLA analysis and Section 3.3 and the other latitude bands and focus on the overall description and the Tokar Gap results, again see discussion below.

I should say that after writing this review I read the comments by the first anonymous reviewer. This person gives a very thorough review, and we have points of agreement and disagreement. I think the major disagreement is how we view the material concerning the Tokar Gap winds and

subsequent eddy spin-up. I really liked this material, but the first reviewer perhaps did not like it so much. I think this is for the authors and the editor to sort out.

Reply:

Thank you very much for your precious comments and suggestions on the manuscript. They were very helpful in improving the manuscript. The reply to specific comments are given below and the manuscript is modified accordingly.

Specific comments:

SC#1:

L40 – I am not sure that “deep water formation” is appropriate. Common usage of that term is for NADW and ABW. Perhaps “intermediate water formation”? At the least tell us how deep this high salinity water reaches.

Reply:

The RSOW is an intermediate water formed in the northern part of Red Sea as part of the convection activity, which propagate through Bab-el-Mandab strait to the Gulf of Aden (Alsaafani & Shenoi 2007) and later spreads to the Indian Ocean, whose signature reaches into the south Indian Ocean about 6000 km away from the source (Beal et al., 2000). The sentence is corrected accordingly.

The earlier text in the manuscript:

It is one of the important deep water formation regions, and its signature reaches into the Indian Ocean (Beal et al., 2000).

The modified text in the manuscript:

It is one of the important intermediate water formation regions in the world (Red Sea Outflow Water, RSOW), formed mainly due to the open ocean convection in the northern Red Sea (Sofianos and Johns, 2003), which propagates through Bab-el-Mandab to the Gulf of Aden (Alsaafani and Shenoi 2007) and later spreads to the Indian Ocean, whose signature reaches into the south Indian Ocean about 6000 km away from the source (Beal et al., 2000).

[Lines: 34-38]

SC#2:

L95 – 1 by 1 degree spacing is very coarse for this region. With such a model can you really expect to resolve the scales that are important in the Red Sea?

Reply:

We have crosschecked the estimates from reanalysis flux products (Tropflux and OAflux) with previous studies in the Red Sea, and found that the variability are consistent with observations (Sofianos and Johns 2003, Murray and Johns 1997, Tragou et al. 1999, Sofianos et al. 2002, Farrar et al. 2009 and Yu and Weller 2007). Further, the variability of the flux parameters (Net heat flux and evaporation. Precipitation is negligible) along the main axis of the Red Sea is relatively smooth, and the general variability can be captured with 1 by 1 degree spacing. Therefore, the Tropflux and the OAflux estimates can be used to understand general variability of these parameters.

In the case of wind, which vary relatively rapid comparing to heat and fresh water flux terms, we have used high resolution winds ($0.312^{\circ} \times 0.312^{\circ}$ spatial grid) from CFSR (Climate Forecast System Reanalysis).

SC#3:

L108-115 – The AVISO SLA is HIGHLY suspect in the Red Sea for resolving eddies. Yes, they grid it at quarter degree spacing, but how much actual data is there? Also, their covariance functions for the OI are not tuned to the Red Sea in general, or to the Tokar Gap in particular. See below, too, but I would remove the AVISO SLA eddy material and focus on the Tokar Gap analysis that doesn't require it.

Reply:

The SLA data from AVISO is used just for a broad and qualitative understanding on the changes in sea level in the Red Sea. We have used the merged data from all satellite estimates. Red Sea has considerable number of satellite tracks from different satellites (Fig.). Further, the AVISO SLA data have been used by previous studies also for the Red Sea region, for example Zhan et al., (2014), Papadopoulos et al., (2015) and Taqi et al., (2017).

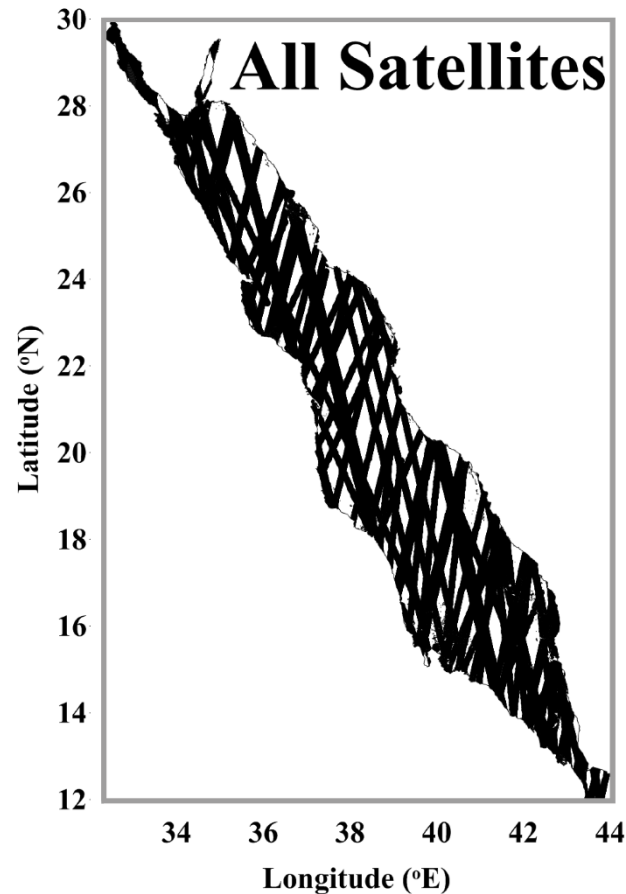


Fig.1 Satellite tracks in the Red Sea.

We agree that a more precise and quantitative estimation of the sea level variability may require further improvements in the AVISO product. But, the SLA data are providing a qualitative understanding of the sea level changes in the Red Sea. We have also compared the geostrophic currents from the hydrographic measurements (profiles collected during different cruises) and from AVISO SLA. Both are matching well. Apart from this, the ADCP measurements carried out by Sofianos and Johns (2007) show the presence of eddies in the

Red Sea, which are well matching with gridded SLA estimates from AVISO for the same period. This gives us confidence to use SLA estimates in the present analysis, at least for a qualitative understanding of the sea level variability.

SC#4:

L122-129 – Well-done to switch to an along-axis coordinate system and to do the analysis in an along-axis, time space. Nice!

Reply:

Thank you for appreciating the work.

SC#5:

L150-162 – I'm worried that we are over-interpreting in this section. The general seasonal pattern is clear, but the along-axis changes are not so clear. Without error bars it is difficult to tell when we are interpreting real changes, or just noise.

Reply:

The error (observed standard deviation from monthly mean value) is mentioned in the text at appropriate locations in the revised manuscript. For the entire climatology, the standard deviation is less than 10 m for >95% cases, while active mixing zone show relatively higher standard deviation.

The observed relatively larger deviation during winter especially in the northern latitudes is due to the measurement of profiles during the ongoing mixing process. In addition, the convection process in the northern Red Sea show considerable interannual variability. This resulted in wide range of MLD values and relatively large standard deviation from the mean value.

The modified text in the manuscript:

A Hovmoller diagram of the monthly MLD climatology is presented in Fig. 3. The deepest MLD is observed in February and the shallowest during May-Jun. A significant annual variability is observed in the Red Sea. The maximum value of climatological mean MLD is observed in February at the northern Red Sea while the minimum noticed at various instances, especially during summer months. The MLD of individual profiles in the northern Red Sea has a wide range values from 40 to 120 m mainly due to the presence of active convection process, while some of the profiles show MLD deeper than 150 m in consistence with Yao et al., (2014). Apart from the northern deep convection region, the south-central Red Sea between 18 °N-21 °N (53 ± 5 m) and 14 °N-16 °N (48 ± 9 m) also experienced deeper MLDs during the winter, which is separated by a shallower MLD around 17 °N (44 ± 14 m). During July to September, the region around 19° N experienced a deeper mixed layer in contrast with the general pattern of summer shoaling over the entire Red Sea.

The deepening of the MLD begins in October throughout the Red Sea. The winter cooling and its associated convection strengthen by December, with an average MLD > 50 m. Compared to other parts 201 of the Red Sea, during November and December, relatively shallower MLDs were witnessed at approximately 16° N-17° N, and 24.5° N-26.5° N. The winter deepening of the MLDs intensifies by January and continues throughout February. In contrast to the general pattern of deeper MLDs in the northern latitudes, the area between 24.5° N and 26.5° N shows a relatively shallow MLD almost throughout the year, especially in the winter.

The mixed layer starts to shoal gradually by the end of February, and the MLDs of most areas decreases to 20 ± 7 m by April. Summer shoaling is comparatively stronger in the 15° N-18° N latitude band, and the detected mean MLD is < 15 m. Individual observations revealed that many profiles have MLDs < 5 m. The area between 24°N and 27°N shows a relatively shallow MLD almost throughout the year, especially during winter.

SC#6:

L160 – As an example of the comment I just made, I cannot make any sense of a “general pattern of deeper MLDs in the latitudes”. I just cannot see in Figure 2 where this statement comes from! You will need to be much more specific to convince me of this and it will also require appropriate error estimates. You lose little by sticking to the bigger picture and skipping the “wiggles”, although the “tongue” at the latitude of the Tokar Gap is interesting (see below).

Reply:

The latitudinal variability in the MLD is clear during winter, with deepest MLD in the north and shallow in the south with deep/shallows in between. Due to this reason, we used the term “general pattern of deeper MLDs in the northern...”. We have removed this part of the sentence from the text.

The earlier text in the manuscript:

In contrast to the general pattern of deeper MLDs in the northern latitudes, the area between 24.5° N and 26.5° N shows a relatively shallow MLD almost throughout the year, especially in the winter.

The modified text in the manuscript:

The area between 24°N and 27°N shows a relatively shallow MLD almost throughout the year, especially during winter.

[Lines: 226-227]

SC#7:

L205 and Figure 5 – I like this plot, but some estimate of the degrees of freedom needs to be made so that we know whether the structure in the curve real or just statistical fluctuations. And, as usual, the degrees of freedom estimate should consider red noise and not assume white, or independent, noise.

Reply:

We have tested the statistical significance of the correlation values. The estimated p-value, t-value and the effective degree of freedom show that the correlation values are significant at 95%. We have tabulated the above stated parameters for a single case (for correlation between NHF and MLD) in the Table given below.

Table.1 Statistics for the correlation between NHF (net heat flux) and MLD.

Latitude (N)	P-value	Effective degree of freedom (timesteps=420. 35*12 months)	t-value based on Bretherton et al, (1999)	t-value for 95% confidence level from "T table"
13	3.20E-09	269.6597	4.842266	1.650517
13.5	0.002644	282.5494	2.477852	1.650256
14	1.38E-06	243.9125	3.726658	1.651123
14.5	5.33E-19	237.3118	7.015846	1.651308
15	3.80E-20	218.1968	6.965186	1.651873
15.5	1.76E-12	174.2134	4.667594	1.653658
16	6.64E-23	219.8966	7.552761	1.651809
16.5	2.61E-32	222.1904	9.367547	1.651746
17	2.53E-56	189.838	12.41162	1.652913
17.5	7.79E-41	182.2344	9.824286	1.653269
18	6.43E-80	163.4437	14.81243	1.654256
18.5	8.99E-47	183.8425	10.77849	1.653177
19	6.06E-45	178.4458	10.34322	1.653459
19.5	2.85E-72	164.7387	13.79153	1.654141
20	5.32E-85	159.815	15.35839	1.654433
20.5	2.37E-86	156.5116	15.38553	1.654617
21	2.27E-74	203.4905	15.67503	1.652394
21.5	3.67E-92	156.3192	16.19286	1.65468
22	7.40E-92	144.0271	15.4933	1.655504
22.5	4.43E-56	204.1266	12.83679	1.652357
23	4.79E-56	237.2501	13.84296	1.651308
23.5	1.15E-65	302.7621	17.48819	1.649898
24	5.63E-112	139.1993	17.98179	1.65589
24.5	1.68E-87	144.9487	14.95348	1.65543

25	4.46E-87	216.5994	18.25168	1.651906
25.5	1.10E-53	218.3447	12.89109	1.651873
26	2.70E-51	128.179	9.546686	1.656845
26.5	6.08E-35	179.0278	8.820048	1.653411
27	1.74E-74	122.4401	12.13284	1.657439
27.5	1.35E-78	151.0859	14.05475	1.655007

SC#8:

L211-215 – I think we are over-interpreting again. These are very small “wiggles” and 2 of the 5 do not even show the pattern you assert, meaning all three curves moving down together. Again, if you want to interpret these small changes, then you have to do a much more thorough job on the statistics to convince us that we’re not just looking at random fluctuations.

Reply:

As mentioned in reply to the previous comment (SC#7), the observed fluctuations are statistically significant at 95% confidence level. The statistical results based on p-value, t-test and degrees of freedom has shown that the parameters (heat flux, freshwater flux and wind stress) correlation coefficients are significant at 95% confidence level.

We have repeated the analysis after smoothing MLD climatology for 1 degree along the latitude and figures are given below.

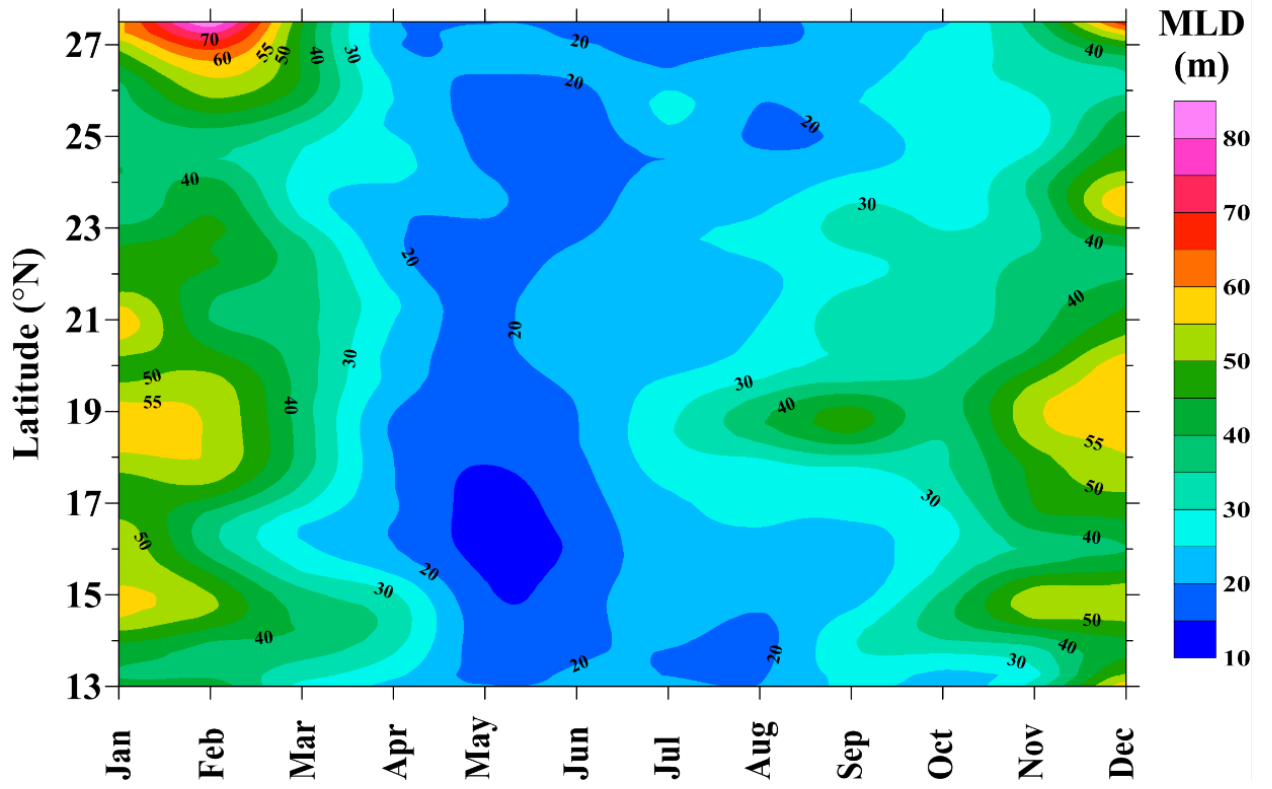


Fig.2 MLD climatology smoothed along latitude for 1 degree.

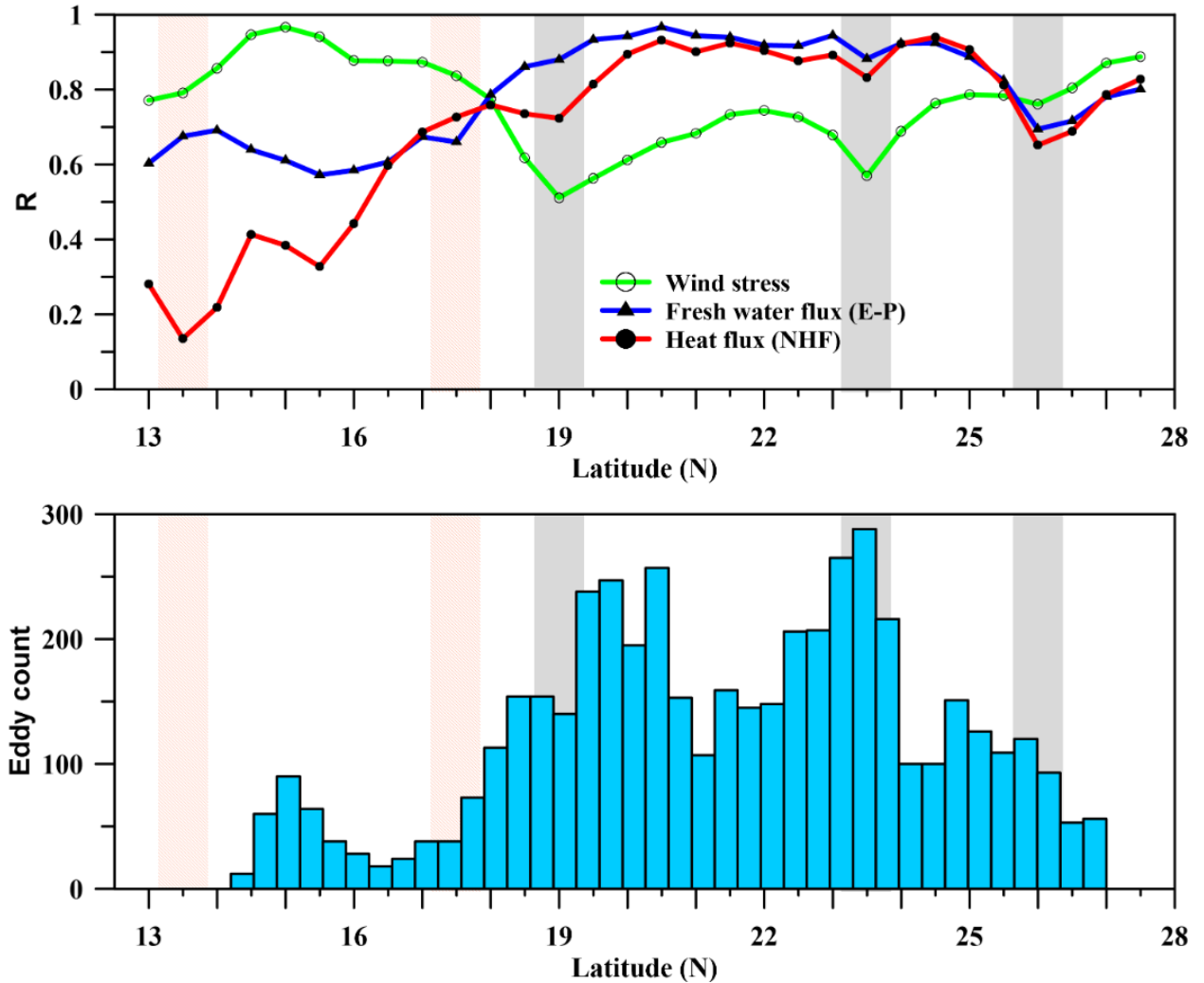


Fig.3 a) The correlation between MLD and atmospheric forces for smoothed MLD climatology, and b) the number of eddies in the Red Sea for the period 1992-2012.

The MLD climatology and correlation curves show a smoothed, but similar structure. A decreasing pattern can be seen correlation values at 19N (clear in wind-stress and heat flux), at 23N (clear in all three forces) and at 26.5N (clear in heat flux and freshwater flux). The correlation drops around 13.5N and 17.5N are less visible. Additionally, a drop around 15N also can be seen associated

Believing that the smoothing may remove some of the small-scale features, we would like to use the original MLD climatology (without smoothing) and previous version of the correlation curve in the manuscript.

SC#9:

L216, all of Section 3.3 – As I mentioned above, the analysis using the AVISO SLA is highly questionable here. I think this entire section, and basically all use of AVISO, is not necessary for this paper. You have some good results, but by pushing too far you run the risk of most readers doubting everything. Please note that I am trying to be constructive here and help to improve the paper. I like the paper as a whole, but really do not like this section.

Reply:

The Sea level anomaly estimate from AVISO is a merged product of multiple satellite tracks. It is true that the research based on SLA has to be carried out with caution, especially in smaller regions like Red Sea. As mentioned in reply to comment SC#3, the Red Sea has considerable number of satellite tracks. Further, multiple studies have already been carried out based on this data. The previous studies show that AVISO SLA estimates can still provide the general picture of sea level changes in the Red Sea. Our study, based on SLA, is only looking to the main locations of eddies in the Red Sea.

SC#10:

L258-260, Figure 6 – This is a continuation of the previous comment. You say that there is a good match with the number of eddies and the latitude ranges you identified earlier from the correlation curves, but I simply do not see that. And since we're just doing the analysis "by eye", then my eye is as good as yours. You really have to do some statistics if you want to make this point. And once again, none of these things are core results of your paper.

Reply:

We agree that few of the correlation drops are not matching with the eddy locations. We have mentioned the same in the manuscript also.

The correlation drops locations matching with eddies:

1. At 19°N: matching with the locations of Tokar region and eddies observed by Zhan et al 2014.
2. At 23°N: matching with eddies observed by Zhan et al 2014.
3. At 26.5°N: matching with eddies observed by Papadopoulos et al., 2015

The correlation drops locations not matching with eddies:

1. At 13.5°N: The Red Sea is very narrow at 13.5°N and close to Bab-el-Mandab strait. Moreover, complex dynamics associated with the exchange of surface and subsurface waters between the Red Sea and the Gulf of Aden occurs in this region. The complexity of this region prevents linking the MLD variability directly to atmospheric forcing or eddies.
2. At 17.5°N: The region at approximately 17.5° N is between the two eddy-driven downwelling zones at approximately 15° N and 19° N (Fig. 2). Mass conservation requires upwelling to replace the downwelling water. The MLD climatology shows shallow mixed layers throughout the year at 17.5° N, which could be due to possible upwelling. Further investigation is required to unveil the dynamics associated with this region.

The drops in correlation at 23°N and 26.5°N are matching with eddy locations. The drop at 19°N is matching with the Tokar region and eddies. indicating the effect of eddies. As mentioned above, the other two locations (13.5°N and 17.5°N) need further investigations to unveil the associated dynamics.

[Lines: 365-379]

SC#11:

L277, all of Section 3.4 – Much better! Looking at the 19N signal where the Tokar Gap is, and showing the actual wind results rather than AVISO eddy counts is much more convincing. And note that this is the only latitude band where I see convincing results. It's well-known that strong winds through mountain gaps generate the eddy signals you infer (search for results on the

Hawaiian Ridge and the Gulf of Tehuantepec), so you do not need the questionable AVISO results in order to rationalize the “tongue” in Figure 2 at 19N. This is a very nice result.

Reply:

Thank you very much for your appreciation.

We agree that mountain gap winds can generate eddy signals in the underlying sea. Therefore, the SLA snapshots are not necessary to show the impact of Tokar winds and associated deepening in MLD to the right of the wind jet and shoaling to the left. We keep SLA maps in figure just for helping the reader to easily understand the position of profiles influenced by mountain gap winds.

References:

1. Al Saafani, M. A., & Shenoi, S. S. C.: Water masses in the Gulf of Aden. *Journal of oceanography*, 63(1), 1-14, 2007.
2. Bretherton, C. S., Widmann, M., Dymnikov, V. P., Wallace, J.M. & Blade, I. The effective number of spatial degrees of freedom of a time-varying field, *J. Clim.*, 12, 1990–2009 (1999).
3. Papadopoulos, V. P., Zhan, P., Sofianos, S. S., Raitzos, D. E., Qurban, M., Abualnaja, Y., Bower, A. S., Kontoyiannis, H., Pavlidou, A., Asharaf, T. T. M., Zarokanellos, N. and Hoteit, I.: Factors governing the deep ventilation of the Red Sea, *J. Geophys. Res. Ocean.*, 120(11), 7493–7505
4. Sofianos, S. S. and Johns, W. E.: Observations of the summer Red Sea circulation, *J. Geophys. Res.* 450 *Ocean.*, 112(6), 1–20, doi:10.1029/2006JC003886, 2007
5. Taqi, A. M., A. M. Al-Subhi & M. A. Alsaafani (2017): Extension of Satellite Altimetry Jason-2 Sea Level Anomalies Towards the Red Sea Coast Using Polynomial Harmonic Techniques, *Marine Geodesy*, DOI: 10.1080/01490419.2017.1333549
6. Zhan, P., Subramanian, A. C., Yao, F. and Hoteit, I.: Eddies in the Red Sea: A statistical and dynamical study, *J. Geophys. Res. Ocean.*, 119(6), 3909–3925, doi:10.1002/2013JC009563, 2014.

Response to short comment#1 (SC#1)

Answer to the review comments from Dr. V M Aboobacker

**Interactive comment on “Mixed layer depth variability in the Red Sea” by Cheriyei P.
Abdulla et al.**

A. Valliyil Mohammed

vmabacker@gmail.com

Received and published: 8 March 2018

The manuscript “Mixed layer depth variability in the Red Sea” discussed the variability by deriving the MLD monthly climatology from temperature profiles. This is probably the first time such a study has been conducted in the Red Sea. The paper is organised well and the discussions are relevant. It forms an important piece of information, especially on the MLD structure and the eddies in the Red Sea. This paper may be accepted in present form for publication in Ocean Science.

A minor comment:

The region around 18 °N experiences the wind convergence during winter. Does it affect the MLD structure in the central Red Sea?

Answer:

Thank you very much for your interest in the manuscript, and for your effort and time in reviewing.

The convergence of wind is observed in the central Red Sea during winter, where NNE winds converge with SSW winds. This resulted in a relatively weak wind speed in the central Red Sea. The climatology of mixed layer in the central Red Sea during this

period has shown relatively deeper mixed layer. It has been observed that the wind convergence during winter result pile up of sea level in the central Red Sea with maximum sea level around 19 °N. This is consistence with results from Sofianos et al., 2001. The pile-up of sea level and possible enhancement in vertical convection could be the reason for relatively deeper mixed layer in the central Red Sea.

Marked-up manuscript

1 **Mixed layer depth variability in the Red Sea**

2 Cheriyei P. Abdulla^{1*}, Mohammed A. Alsaafani^{1,2}, Turki M. Alraddadi¹, and Alaa M. Albarakati¹

3 ¹Department of Marine Physics, Faculty of Marine Sciences, King Abdulaziz University, Jeddah, Saudi Arabia.

4 ²Department of Earth & Environmental Sciences, Faculty of Science, Sana'a University, Yemen.

5

6 *Correspondence to:* Cheriyei P. Abdulla (acp@stu.kau.edu.sa)

7 **Abstract**

8 For the first time, a monthly climatology of mixed layer depth (MLD) in the Red Sea has been derived
9 based on temperature profiles. The general pattern of MLD variability is clearly visible in the Red Sea,
10 with deep MLDs during winter and shallow MLDs during summer. Transitional MLDs have been found
11 during the spring and fall. Northern end of the Red Sea experienced deeper mixing and higher MLD,
12 associated with the winter cooling of the high-saline surface waters. Further, the region north of 19° N
13 experienced deep mixed layers, irrespective of the season. Wind stress plays a major role in the MLD
14 variability of the southern Red Sea, while net heat flux and evaporation are the dominating factors in the
15 central and northern Red Sea regions. Ocean eddies and Tokar gap winds significantly alters the MLD
16 structure in the Red Sea. The dynamics associated with the Tokar gap winds leads to a difference of more
17 than 20 m in the average MLD between the north and south of the Tokar axis.

18 **Keywords:** Mixed layer depth, Red Sea, Eddies, Tokar gap winds, Air-Sea interaction.

19 **1 Introduction**

20 The surface mixed layer is a striking and universal feature of the open ocean where the turbulence
21 associated with various physical processes leads to the formation of a quasi-homogeneous layer with
22 nearly uniform properties. The thickness of this layer, often named mixed layer depth (MLD), is one of
23 the most important oceanographic parameters, as this layer directly communicates and exchanges energy
24 with the atmosphere and therefore has a strong impact on the distribution of heat (Chen et al., 1994),
25 ocean biology (Polovina et al., 1995) and near-surface acoustic propagation (Sutton et al., 2014). Heat
26 and fresh-water exchanges at the air-sea interface and wind stress are the primary forces behind turbulent
27 mixing. The loss of heat and/or freshwater from the ocean surface can weaken the stratification and
28 enhance the mixing. Similarly, a gain in heat and/or freshwater can strengthen the stratification and reduce
29 the mixing. The shear and stirring generated by the wind stress enhance the vertical mixing and play a
30 major role in controlling the deepening of the oceanic mixed layer. Further, the stirring associated with
31 turbulent eddies predominantly changes the mixing process, mainly along the isopycnal surfaces where
32 stirring may occur with minimum energy (de Boyer Montegut et al., 2004; Hausmann et al., 2017; Kara
33 et al., 2003).

34 It is one of the important intermediate water formation regions in the world (Red Sea Outflow Water,
35 RSOW), formed mainly due to the open ocean convection in the northern Red Sea (Sofianos and Johns,
36 2002), which propagates through Bab-el-Mandab to the Gulf of Aden (Alsaafani and Shenoi, 2007) and
37 later spreads to the Indian Ocean, whose signature reaches into the south Indian Ocean about 6000 km
38 away from the source (Beal et al., 2000). The Red Sea is surrounded by extremely hot arid lands and has
39 a relatively strong evaporation rate (2 m yr^{-1}) with nearly zero precipitation (Albarakati and Ahmad, 2013;
40 Bower and Farrar, 2015; Sofianos et al., 2002). This region experiences strong seasonality in its
41 atmospheric forcing and buoyancy. These characteristics, along with the lack of river input, make the Red
42 Sea one of the hottest and most saline ocean basin in the world. The narrow and semi-enclosed nature of
43 the basin, the presence of multiple eddies, strong evaporation, lack of river input and very weak
44 precipitation, seasonally reversing winds, etc. lead to complex dynamical processes in the Red Sea
45 (Aboobacker et al., 2016; Yao et al., 2014a, 2014b; Zhai and Bower, 2013; Zhan et al., 2014).

Deleted: The Red Sea is a semi-enclosed narrow basin connected to the Indian Ocean through the Gulf of Aden. It is one of the important deep water formation regions, and its signature reaches into the Indian Ocean (Beal et al., 2000)

50 The increase in number temperature and salinity profiles in recent years enhanced the study of MLD
51 structure and its variability, both globally (de Boyer Montegut et al., 2004; Kara et al., 2003; Lorbacher
52 et al., 2006) and regionally (Abdulla et al., 2016; D’Ortenzio et al., 2005; Keerthi et al., 2012, 2016; Zeng
53 and Wang, 2017). The Red Sea has been investigated for many years with an emphasis on its different
54 physical features. But, no detailed investigation on MLD variability has been documented so far in the
55 Red Sea, except few studies addressing the hydrography and vertical mixing of localized areas (Alsaafani
56 and Shenoi, 2004; Bower and Farrar, 2015; Carlson et al., 2014; Yao et al., 2014b).

57 In this work, an MLD climatology is produced for the first time based on in situ observations. Further,
58 the roles of atmospheric forces and oceanic eddies on the changes of the MLD have been investigated.
59 The following sections are arranged as: Sect. 2 describes the datasets used and methodology. The
60 subsequent sections discuss the observed MLD variability in the Red Sea (Sect. 3), the role of the major
61 forces on the MLD variability (Sect. 4), the impact of eddies on MLD changes (Sect. 5) and the influence
62 of Tokar gap winds (Sect. 6). The main conclusions of the present work are given in the final section.

63 **2 Data and methods**

64 **2.1 Datasets**

65 Temperature and salinity profiles from different sources are collected, which are measured using CTD
66 (conductivity-temperature-density profiler), PFL (autonomous profiling floats including ARGO floats),
67 XBT (expendable-bathy-thermograph) and MBT (mechanical-bathy-thermograph). The World Ocean
68 Database (<https://www.nodc.noaa.gov/OC5/SELECT/dbsearch/dbsearch.html>) is the main source with
69 larger number of profiles. Apart from this, data from Coriolis data center
70 (<http://www.coriolis.eu.org/Data-Products/Data-Delivery/Data-selection>) and several cruises conducted
71 by individual institutions are also used in this analysis. The bathythermograph profiles were depth-
72 corrected based on Cheng et al., (2014). A total 13,891 temperature profiles were made for the Red Sea
73 (approximately 14 % of these profiles have salinity measurements) from 1934 to 2017.

74 These profiles are quality checked according to the procedure given in Boyer and Levitus (1994). In the
75 duplicate check, all the profiles within a 1 km radius and taken on the same day are considered duplicates
76 and are removed from the main dataset. The levels in the profile with large inversions in temperature
77 (inversion $\geq 0.3^\circ\text{C}$) are flagged and removed. If three or more inversions are present, then the entire
78 profile is removed. The levels with extreme gradients $\geq 0.7^\circ\text{C}$ are also removed from the profile. Since
79 the present work is more focused on the changes in the upper layer of the ocean (from the surface to a
80 150 m depth), profiles with low resolutions in the upper layers are removed. Almost 50 % of the profiles
81 have resolutions of < 5 m, while 7 % of the profiles have poor resolutions (resolutions of > 25 m).

Deleted: The number of profiles removed at each step of the quality check is tabulated in Table S1.

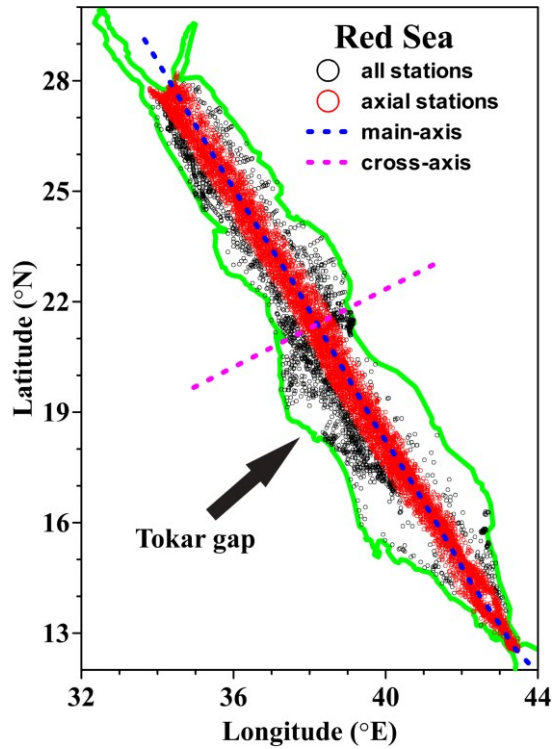
82 [Out of the total of 13,891 profiles analysed, 11,212 profiles passed the quality check from CTD \(690\),](#)
83 [PFL \(1385\), XBT \(5507\) and MBT \(3630\), and the spread is shown in Fig. 1.](#) More than 80 % of these
84 profiles are positioned along the middle of the Red Sea, with a sufficient number of profiles for each
85 month ([Fig. S1](#)). The yearly and monthly distributions of the temperature profiles lie along the middle of
86 the Red Sea and are given in the supplementary material ([Fig. S2-S3](#)). As part of the quality check, 2679
87 profiles were removed from the main dataset. A total of 2063 salinity profiles are available for the entire
88 Red Sea ([Fig. S4](#)). MLD is estimated based on the temperature profiles due to the increased number and
89 sufficient monthly coverage comparing to that of salinity. The [distribution](#) of the temperature profiles
90 used in this analysis is shown in [Fig. 1](#).

Deleted: A total of 11,212 profiles passed the quality check from CTD (690), PFL (1385), XBT (5507) and MBT (3630), and the spread is shown in Fig. 1.

Deleted: Tables 2-3

Deleted: Table 4

Deleted: spread



99

100 **Figure 1.** The locations of temperature profiles in the Red Sea. Black circles denote all available profiles,
 101 while red circles denote the profiles close to the main-axis that used for climatology calculation. The blue
 102 (magenta) dashed line indicate main-axis (cross-axis) of the Red Sea.

103 The monthly mean values of heat fluxes and wind stress data are provided by Tropflux at a $1^\circ \times 1^\circ$ spatial
 104 resolution for the period 1979-2016, which are used to check the influence on MLD variability
 105 (http://www.incois.gov.in/tropflux_datasets/data/monthly/). Tropflux captures better variability and less
 106 bias than the other available fluxes and wind stress products (Praveen Kumar et al., 2012, 2013). Since
 107 evaporation is not provided by Tropflux, the monthly mean values of evaporation from OAflux (from

108 1979 to 2016 and 1°x1° spatial resolution) are used
109 (ftp://ftp.who.i.edu/pub/science/oaflux/data_v3/monthly/evaporation/). The TRMM (Tropical rainfall
110 measuring mission, <https://pmm.nasa.gov/data-access/downloads/trmm>) satellite provided the
111 precipitation information for every 0.25°x0.25° grid and 3-hourly to monthly time scale from 1997 to
112 2016 (TRMM monthly 3B43_V7 product is used). Monthly climatology of heat flux, evaporation,
113 precipitation and wind stress are calculated. The period of precipitation data used for climatology
114 calculation is shorter than other parameters. The present analysis is focusing on the seasonal timescale,
115 and [therefore](#), shorter data period will not significantly affect the results.

116 The daily sea level anomaly (SLA) maps are provided by AVISO (www.aviso.oceanobs.com). These data
117 are the merged product of satellite estimates from TOPEX/Poseidon, Jason-1, ERS-1/2, and Envisat and
118 are globally available for every 0.25°x0.25° grid from the year 1992 to present (Ducet et al., 2000;
119 LaTraon and Dibarboure, 1999). The SLA maps are used to describe the eddy distribution in the Red Sea.
120 Climate Forecast System Reanalysis (CFSR) provided hourly wind product from 1979 to 2010 at every
121 0.312°x0.312° grid (<https://rda.ucar.edu/datasets/ds093.1/#!access>) which is validated in the Red Sea by
122 Aboobacker et al., (2016). CFSR hourly wind at 10 m above the surface is used to study the Tokar gap
123 winds.

124 2.2 Methods

125 [The MLD can be estimated based on different methods. The Fig.2 shows a sample temperature profile](#)
126 [collected on 19th January 2015 from Red Sea \(24.9° N, 35.18 °E\), with short-range gradients within the](#)
127 [mixed layer. This gradient could rise from instrumental errors or turbulence in the upper layer. The](#)
128 [curvature method](#) (Lorbacher et al., 2006) [identified MLD at 32 m, due to the presence of a short-range](#)
129 [gradient at this depth.](#) The threshold method (de Boyer Montegut et al., 2004) [detected MLD at 130 m](#)
130 [\(threshold = 0.2 °C\), while the segment method](#) (Abdulla et al., 2016) [identified MLD at 120 m. The](#)
131 [segment method based MLD could be considered as a reliable estimate comparing to both curvature](#)
132 [\(underestimation\) and threshold method \(overestimation\). The segment method first identifies the portion](#)
133 [of the profile with significant inhomogeneity where the transition from a homogeneous layer to](#)

Deleted:

Deleted:

inhomogeneous layer occurs. Then, this portion of the profile is analyzed to determine the MLD (detailed procedure of the estimation technique is given Abdulla et al., 2016). In the present study, MLD is estimated based on the segment method, which is found to be less sensitive to short-range disturbances within the mixed layer (Abdulla et al., 2016). This method first identifies the portion of the profile (segment) where the transition from a homogeneous layer to inhomogeneous layer occurs. Then, this segment is analyzed to determine the MLD.

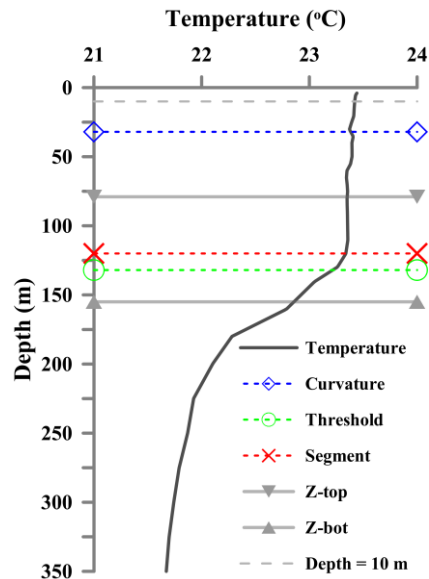


Figure 2. The MLD estimated for a sample temperature profile based on curvature, threshold, and segment methods. The Z-top and Z-bot respectively represent the top and bottom ends of the portion of the profile with significant inhomogeneity.

Deleted: Different approaches are available for MLD estimation. The MLD calculated based on three methods for a schematic temperature profile is shown in Fig. 2. Short-range gradients are manually inserted at different depths within the mixed layer, which can be expected from instrumental errors or due to turbulence in the upper layer. The threshold method (de Boyer Montégut et al., 2004) detected MLD at 26 m depth (threshold = 0.2 °C), while curvature method (Lorbacher et al., 2006) identified MLD at ~10 m. The segment method (Abdulla et al., 2016) identified MLD at 120 m, which could be considered as a reliable estimate comparing to both curvature and threshold method. The segment method first identifies the portion of the profile with significant inhomogeneity where the transition from a homogeneous layer to inhomogeneous layer occurs. Then, this portion of the profile is analysed to determine the MLD (detailed procedure of the estimation technique is given Abdulla et al., 2016). In the present study, MLD is estimated based on the recently introduced segment method, which is found to be less sensitive to short-range disturbances within the mixed layer (Abdulla et al., 2016). This method first identifies the portion of the profile (segment) where the transition from a homogeneous layer to inhomogeneous layer occurs. Then, this segment is analyzed to determine the MLD.

Deleted: s

170 The availability of profiles is denser along the middle of Red Sea during all months. The present analysis
171 is performed for the profiles that fall within 0.5 degrees to the east and west of the main axis that, running
172 along almost the middle of the Red Sea (hereafter called the “main axis”), has the advantage of a sufficient
173 number of profiles for every month. The main axis of the Red Sea is inclined to the west, with respect to
174 true north, by ~30 degrees. For this reason, instead of zonally averaging, the climatology is calculated by
175 averaging the MLDs in an inclined direction parallel to the “cross-axis” (Fig. 1). The MLD is estimated
176 for the individual profiles, and then, the monthly climatology is calculated every 0.5° from south to north
177 (13 °N to 27.5 °N).

Deleted:

Deleted:

178 The heat flux, evaporation, precipitation and wind stress are interpolated to 0.5°x0.5° spatial grid to match
179 with MLD climatology with the help of climate data operator (CDO) tool available at
180 <http://www.mpimet.mpg.de/cdo>. The change in surface water buoyancy forces is calculated following
181 (Turner, 1973)

Deleted: s

$$182 \quad B_0 = (C_p^{-1} g \alpha \rho_0^{-1} Q_{net}) + (-1 * g \beta s (E - P)) = B_{0T} + B_{0H} \quad (1)$$

183 where C_p = water heat capacity, g = acceleration due to gravity, α =thermal expansion coefficient, ρ_0 =
184 density of surface water, Q_{net} = net heat flux at the sea surface, β = haline contraction coefficient, s =salinity
185 of surface water, E = evaporation rate, and P = precipitation. In Eq. (1), B_{0T} and B_{0H} , respectively, represent
186 the thermal and haline components of the buoyancy force. For ease of explanation, the Red Sea is divided
187 into southern (13° N-18° N), central (18° N-23° N) and northern (23° N-28° N) regions and the seasons
188 defined as winter (Dec-Feb), spring (Mar-Apr), summer (May-Aug) and fall (Sep-Nov).

189 3 Results and discussion

190 3.1 MLD variability in the Red Sea

191 The Red Sea exhibits strong seasonal changes in its MLD, with deeper mixed layers during the winter
192 and shallower ones during the summer, with gradual changes from deeper to shallower and vice versa in
193 the transitional months. [A Hovmoller diagram of the monthly MLD climatology is presented in Fig. 3.](#)

The deepest MLD is observed in February and the shallowest during May-Jun. A significant annual variability is observed in the Red Sea. The maximum value of climatological mean MLD is observed in February at the northern Red Sea while the minimum noticed at various instances, especially during summer months. The MLD of individual profiles in the northern Red Sea has a wide range values from 40 to 120 m mainly due to the presence of active convection process, while some of the profiles show MLD deeper than 150 m in consistence with Yao et al., (2014). Apart from the northern deep convection region, the south-central Red Sea between 18 °N-21 °N (53+/-5 m) and 14 °N-16 °N (48+/-9 m) also experienced deeper MLDs during the winter, which is separated by a shallower MLD around 17 °N (44+/-14 m). During July to September, the region around 19° N experienced a deeper mixed layer in contrast with the general pattern of summer shoaling over the entire Red Sea.

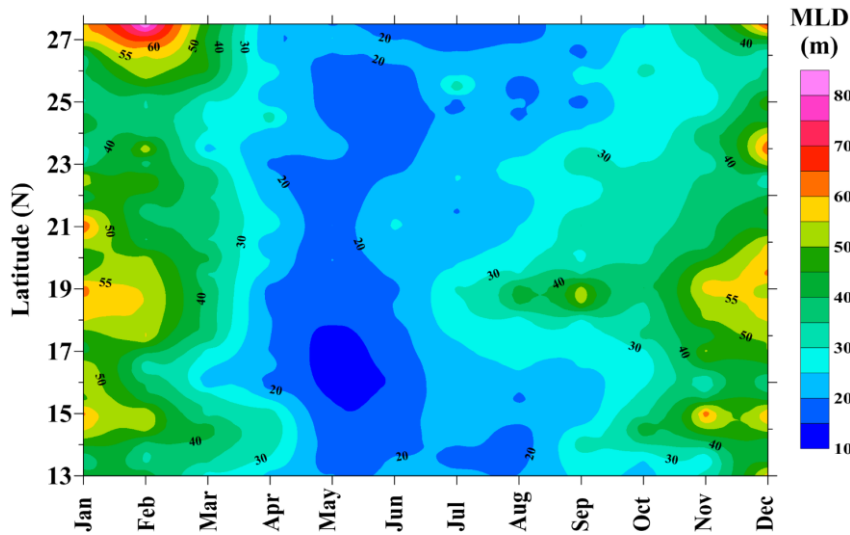


Figure 3. Hovmöller diagram of the MLD climatology along the axis of Red Sea.

Deleted: A Hovmöller diagram of the monthly MLD climatology is presented in Fig. 2. The deepest MLD is observed in February; the shallowest, during May-Jun. A significant annual variability is observed in the Red Sea. The maximum value of climatological mean MLD is observed in February at the northern Red Sea while the minimum noticed at various instances, especially during summer months. The MLD of individual profiles in the northern Red Sea has a wide range values from 40 to 120 m mainly due to the presence of active convection processes, while some of the profiles show MLD deeper than 150 m. Numerical simulations by Yao 2014 winter, Osipov 2017 also reported similar results. Apart from the northern deep convection region, the south-central Red Sea (14° N-21° N) also experienced deeper MLDs during the winter, with mean MLD 60+/-13 m. In contrast to the general pattern of shoaling during the summer, the region around 19° N experienced a deeper mixed layer from July to September.

226 The deepening of the MLD begins in October throughout the Red Sea. The winter cooling and its
227 associated convection strengthen by December, with an average MLD > 50 m. Compared to other parts of
228 the Red Sea, during November and December, relatively shallower MLDs were witnessed at
229 approximately 16° N-17° N, and 24.5° N-26.5° N. The winter deepening of the MLDs intensifies by
230 January and continues throughout February. [The area between 24°N and 27°N shows a relatively shallow](#)
231 [MLD almost throughout the year, especially during winter.](#)

232 The mixed layer starts to shoal gradually by the end of February, and the MLDs of most areas decrease
233 to 20±7 m by April. Summer shoaling is comparatively stronger in the 15° N-18° N latitude band, and
234 the detected mean MLD is < 15 m. Individual observations revealed that many profiles have MLDs < 5
235 m. In general, the shallow mixed layers are predominant from April to September, while this prevails
236 until October in the far north. In the south-central Red Sea, the shallow mixed layer exists for only a short
237 period, from April to June.

238 3.2 Major forces controlling the MLD variability

239 MLD is directly influenced by changes in the net heat flux (NHF), fresh-water flux (E-P) and wind stress.
240 The different terms that contribute to NHF are given in [Fig. 4](#) for a sample year 2016 in the central Red
241 Sea. On an annual average basis, the incoming shortwave radiation (SWR, 202 W m⁻², positive
242 downward) is mainly balanced by LHF (latent heat flux, -126 W m⁻²) and LWR (long wave radiation, -
243 83 W m⁻²), while the SHF (sensible heat flux) is only -4 W m⁻². The net heat loss in the central Red Sea
244 is 11 W m⁻². Both the LHF and LWR are gradually increasing towards the northern Red Sea. The monthly
245 climatology of the NHF in the northern, central and southern Red Sea are given in [Fig. 5a](#). Heat loss rises
246 above 200 W m⁻² during December-January in the northern Red Sea, with a maximum of ~250 W m⁻² at
247 the northern end of the sea in December. The annual mean of NHF is negative (heat loss) across the Red
248 Sea, except for isolated locations in the southern Red Sea with trivial heat gain (figure not shown). The
249 thermal components of the buoyancy forces calculated based on Eq. (1) show that the heat flux [support](#)
250 [mixing through buoyancy loss](#) in the northern and central Red Sea during the winter, while it [opposes](#)

Deleted: In contrast to the general pattern of deeper MLDs in the northern latitudes, the area between 24.5° N and 26.5° N shows a relatively shallow MLD almost throughout the year, especially in the winter. ¶

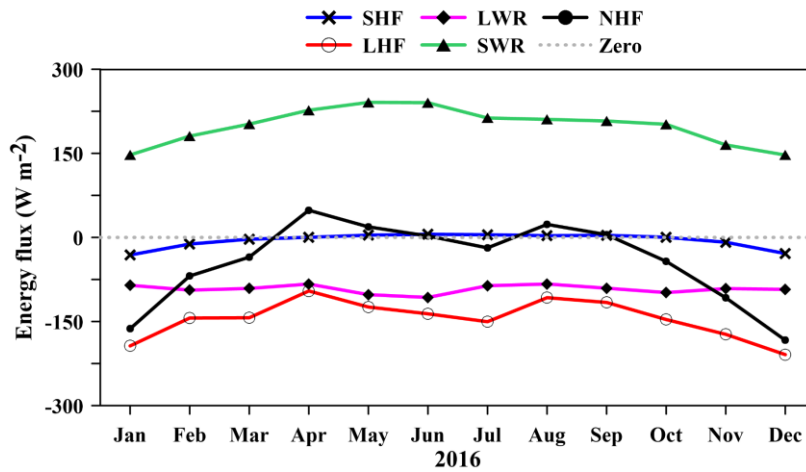
Deleted: e

Deleted: enhance

Deleted: slightly

258 [vertical](#) mixing [due to buoyancy gain](#) during summer. In the southern Red Sea, the effect of heat flux is
259 relatively weak.

Deleted: diminishes

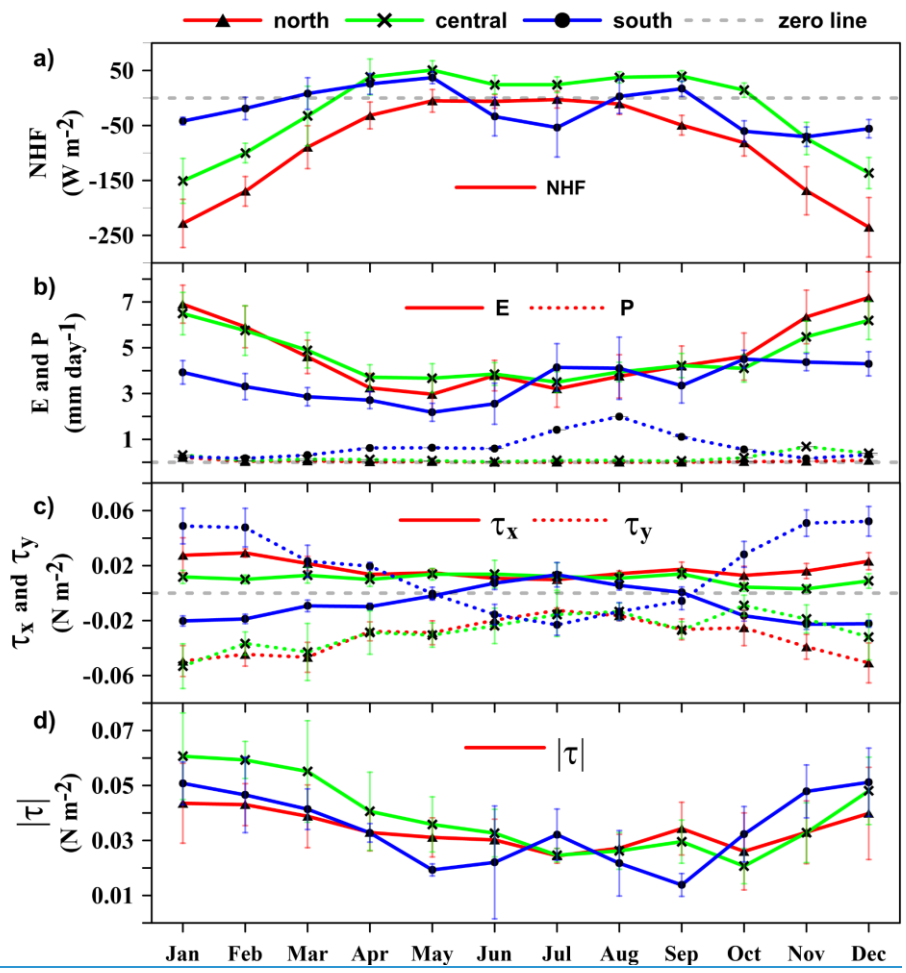


260

261 **Figure 4.** Time series of heat flux components ([incoming shortwave radiation \(SWR\)](#), [long wave](#)
262 [radiation \(LWR\)](#), [latent heat flux \(LHF\)](#), [sensible heat flux \(SHF\)](#) and [net heat flux \(NHF\)](#)) for the year
263 2016 in the central Red Sea.

264 The evaporation rate in the Red Sea gradually increases from south to north ([Fig. 5b](#)). The central and
265 northern Red Sea have higher evaporations during the winter ($\sim 6 \text{ mm day}^{-1}$) and moderate evaporations
266 ($\sim 3 \text{ mm day}^{-1}$) during the summer. Evaporation shows weak seasonality in the southern Red Sea.
267 Precipitation in the southern region is higher than those of the other areas of Red Sea, with maximum
268 rainfall during July-September ([Fig. 5b](#)). The changes in buoyancy forces corresponding to fresh-water
269 flux (haline component) are estimated based on Eq. (1), which shows that the changes support [vertical](#)
270 mixing throughout the year and over the entire Red Sea. The thermal component is relatively higher than
271 the haline component, and the net buoyancy [flux](#) follows a more or less similar pattern of thermal
272 buoyancy [flux](#) all along the Red Sea (figure not shown). The observed variability of the above-discussed

274 parameters is consistent with findings from earlier studies (Albarakati and Ahmad, 2013; Sofianos et al.,
 275 2002; Tragou et al., 1999).



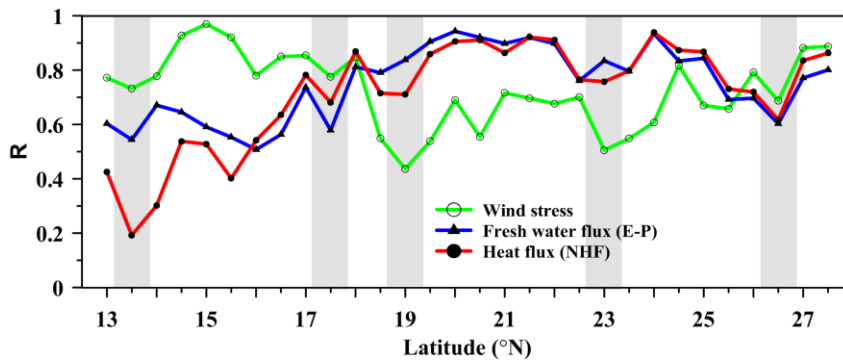
276

277 **Figure 5.** Monthly climatology of a) NHF, b) evaporation and precipitation, c) eastward (τ_x) and
 278 northward (τ_y) component of wind-stress, and d) magnitude of the wind stress ($|\tau|$), South, central and
 279 north regions are represented by the changes at 14° N, 21° N and 27° N.

Deleted: , and c) wind stress.

280 The pattern of wind stress in the Red Sea is significantly different from the other parameters. The wind
 281 stress is strong during the winter, leading to enhanced turbulence and mixing, while it is weak during the
 282 summer, resulting in a shallower mixed layer (Fig. 5c,d). Apart from that, strong surface winds blow to
 283 the Red Sea through the Tokar gap at approximately 19°N in July and August.

Deleted:



285 **Figure 6.** Correlation between major forces and MLD. Shaded regions represent locations of coinciding
 286 drops in correlation.

287 The correlations between MLDs and forcing factors are given in Fig. 6. The wind stress and E-P are
 288 positively correlated with MLD while the NHF is negatively correlated since as NHF (into the ocean)
 289 increases, MLD decreases. For simplicity of the figure (Fig. 6), the correlation values of all parameters
 290 are presented as positive. NHF and E-P are well correlated (>0.8) with MLD in the central and northern
 291 Red Sea, and weakly correlated in the south. Wind stress has a higher correlation (>0.8) to the south,

Deleted: Variability in MLD has an opposite phase to that of NHF, while the rest of the forcing are linearly phase related.

296 while it is relatively weakly correlated in the central and northern Red Sea. Toward the northern end, the
297 wind stress gradually achieves a higher correlation.

298 The results from [Fig. 5](#) and [6](#) indicate that the MLD variability of the Red Sea is dominated by wind stress
299 in the southern part, NHF (heat flux) and evaporation play a major role in the central region, while all the
300 three are influencing in the northern region. Remarkably, for all the above-discussed parameters,
301 coinciding drops are observed in the correlations at approximately 13.5° N, 17.5° N, 19° N, 23° N, and
302 26.5° N. These drops are discussed in the following section.

303 3.3 Impact of [the eddies](#)

304 Satellite altimetry maps revealed the presence of [multiple eddies](#) in the Red Sea which are often confined
305 to specific latitude bands. Quadfasel and Baudner (1993) reported that most of the gyres in the Red Sea
306 are concentrated in four latitude bands, approximately centered on 18° N, 20° N, 23° N and 26.5° N, and
307 some of these eddies are semi-permanent in nature. Johns et al. [\(1999\)](#) also reported [the presence of](#)
308 cyclonic eddies in the north and south of the Red Sea and anticyclonic eddies in the central Red Sea.
309 Clifford et al. (1997) and Sofianos and Johns (2007) reported the presence of a quasi-permanent cyclonic
310 gyre in the northern Red Sea during the winter. Analyzing the SLA maps from 1992 to 2012, Zhan et al.,
311 (2014) reported the presence of [multiple eddies](#) with both polarities in the Red Sea. The number of
312 identified eddies peaked at approximately 19.5° N and 23.5° N. The upwelling proxy constructed using
313 MODIS SST in the northern Red Sea shows the presence of frequent upwelling events at approximately
314 26.5° N almost every year (Papadopoulos et al., 2015) indicating [the presence of cyclonic eddy](#). The
315 extent and time of the upwelling vary from year to year.

316 The eddy distribution in the Red Sea for the period from 1992-2012, based on SLA data is given in [Fig.](#)
317 [7, where the eddies are identified using the “winding-angle” method \(Zhan et al., 2014\)](#). The number of
318 eddies are relatively higher in the central and northern Red Sea. The change in vertical stratification due
319 to the presence of anticyclonic eddy (AE) and cyclonic eddy (CE) for different seasons are shown in [Fig.](#)
320 [8](#). The black (green) colored curve represent the profile before (during) the eddy event. The date of
321 profiling is given in the figure caption and the stations are marked. Figure 7a & 7f shows that the presence

Deleted: a

Deleted: (1999)

Field Code Changed

Deleted: Johns et al.,

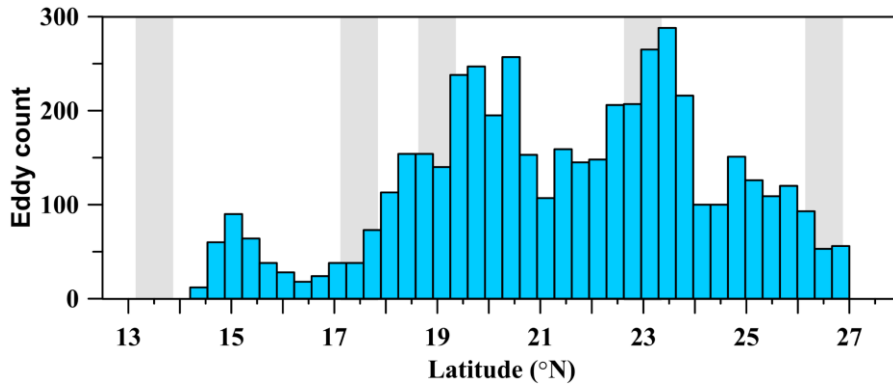
Deleted: a

Deleted: .

327 of AE during spring transformed the completely stratified upper layer to be well mixed till 50 m depth.
328 Similar instance is shown in [Fig. 8b](#) & [8g](#) where MLD changed from nearly zero to 30 m during summer.
329 Figure 7c & 7h show the profiles corresponding to a CE event during fall, where shoaling of MLD by
330 ~10 m is observed. Similarly, the CE event during winter lead to shoaling of mixed layer by ~60 m ([Fig.](#)
331 [8d](#) & [8i](#)). Figure [8e](#) & [8j](#) show three profiles from single cruise collected within 12 hours which is
332 coincided with the presence of CE and AE in a short distance, in which station A is located outside the
333 AE, B is located inside AE and C is partly in CE. There is a difference of ~100 m in the MLD due to the
334 presence of eddies, in a short distance. Similarly, the MLD at station C is shallower than that of A due to
335 the presence of a CE.

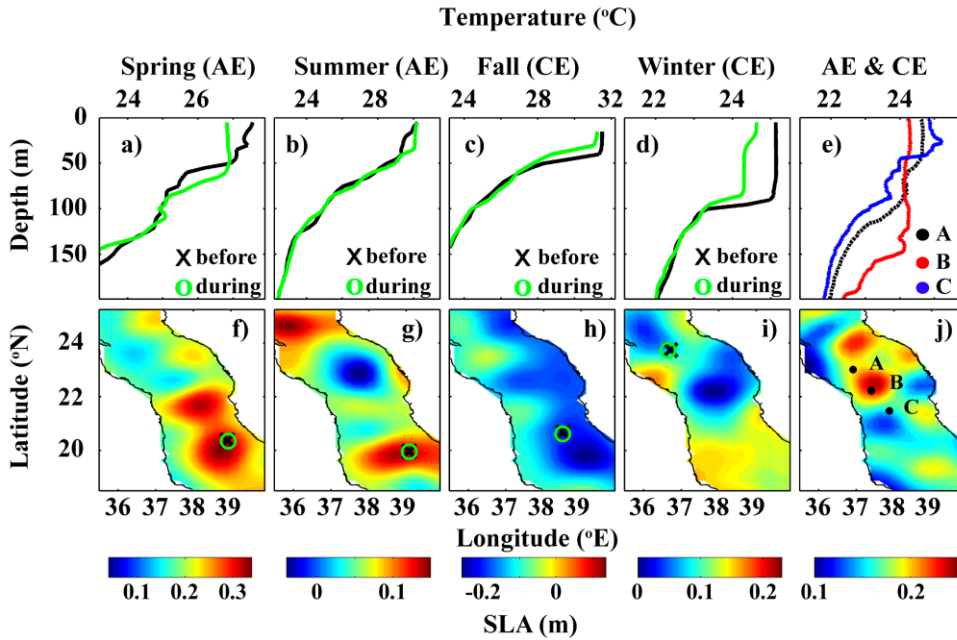
336 [Previous studies have proved that the upper ocean is efficiently re-stratified by the ocean eddies which](#)
337 [may significantly change the MLD. The resultant effect of eddy is largely dependent on the eddy](#)
338 [amplitude. The mixing intensity is largest at the center of eddy and decays on average with increasing](#)
339 [radial distance](#) (Dewar, 1986; Fox-Kemper et al., 2008; Hausmann et al., 2017; Smith and Marshall,
340 2009). [The observed results show that the mixing associated with eddies is dominating over the existing](#)
341 [effect of wind stress and heat flux. CE diminishes mixing through upwelling of the subsurface water while](#)
342 [AE enhances mixing through downwelling of the surface water](#) (de Boyer Montégut et al., 2004; Chelton
343 et al., 2004, 2011; Dewar, 1986; Hausmann et al., 2017).

Deleted: Previous researches have been proved that the upper ocean is efficiently restratified by the ocean eddies which may significantly change the MLD. The resultant effect of eddy is largely dependent on the eddy amplitude. The mixing intensity is largest at the centre of eddy and decay on average with increasing radial distance (Dewar, 1986; Fox-Kemper et al., 2008; Hausmann et al., 2017; Smith and Marshall, 2009). The CE diminishes mixing through the upwelling of the subsurface waters, while an AE enhances mixing through the downwelling of the surface waters (de Boyer Montégut et al., 2004; Chelton et al., 2004, 2011; Dewar, 1986; Hausmann et al., 2017).



356

357 **Figure 7.** The number of eddies in the Red Sea derived from sea level anomaly for the period 1992-2012.
 358 The eddy count values are taken from Zhan et al., 2014. Shaded regions represent the location of
 359 correlation drops as shown in [Fig. 6](#).



360

361 **Figure 8.** Profiles collected during (a) spring, (b) summer, (c) fall and (d) winter from the nearby stations
 362 in the Red Sea. The stations are marked on the SLA maps of the corresponding days (f-i). The “x” mark
 363 (“o” mark) represent profile collected before the appearance of the eddy (during the eddy period) and
 364 plotted in black (green) color. The dates of black and green profiles are respectively c) 11-03-2016 & 18-
 365 03-2016, e) 06-06-2016 & 13-06-2016, g) 16-09-2010 & 21-09-2010 and i) 13-12-2015 & 17-12-2015.
 366 The SLA is averaged for 5 days prior to the date of the later (green) profile. e) Temperature profiles
 367 collected from stations A, B & C within 12 hours (6th-7th Feb 2005) and j) the average SLA map for the
 368 period 4th to 7th Feb 2005.

369 The coinciding drops in the correlation curves, observed at approximately 19° N, 23° N and 26.5° N are
 370 well matching with the main eddy locations (Bower and Farrar, 2015; Johns et al., 1999; Quadfasel and

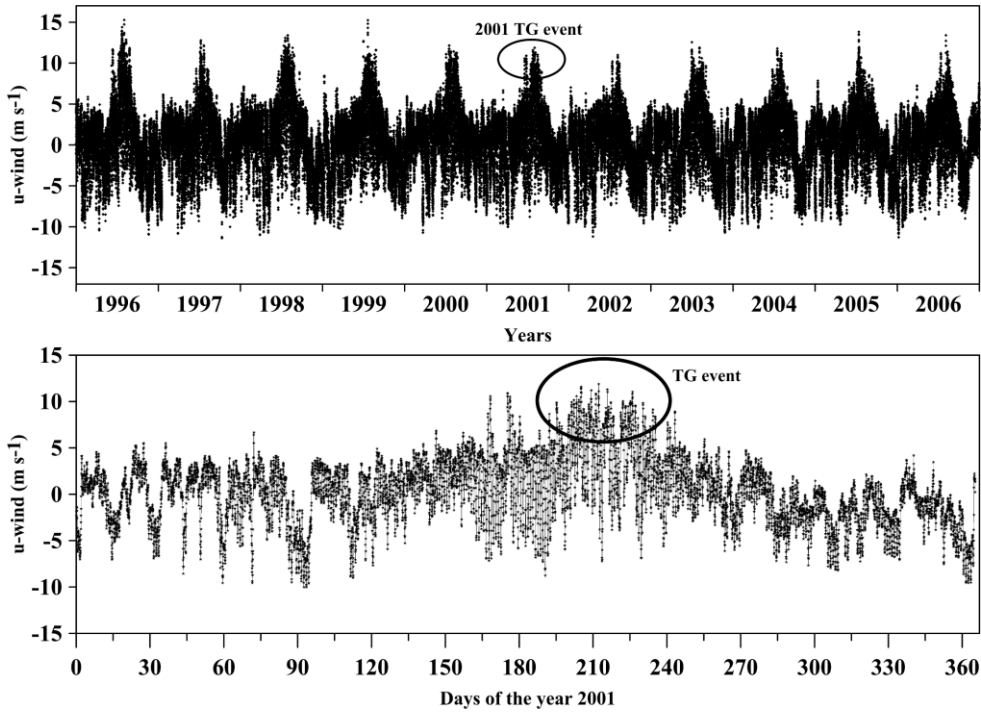
371 Baudner, 1993; Zhai and Bower, 2013; Zhan et al., 2014), while those of 13.5° N and 17.5° N are not
372 (Fig. 6 and 7). The Red Sea is very narrow at 13.5° N. Moreover, complex dynamics associated with the
373 exchange of surface and subsurface waters between the Red Sea and the Gulf of Aden occur in this region.
374 The complexity of this region prevents linking the MLD variability directly to atmospheric forcing or
375 eddies. The region at approximately 17.5° N is between the two eddy-driven downwelling zones at
376 approximately 15° N and 19° N (Fig. 3). Mass conservation requires upwelling to replace the
377 downwelling water. The MLD climatology shows shallow mixed layers throughout the year at 17.5° N,
378 which could be due to possible upwelling. Further investigation is required to unveil the dynamics
379 associated with this region.

380 Rapid shoaling of the mixed layer is seen at ~26.5° N over a short distance (~100 km) adjacent to the
381 deep convection zone in the northern side. The presence of a quasi-permanent cyclonic gyre during the
382 winter (Clifford et al., 1997; Sofianos and Johns, 2007) and frequent upwelling events (Papadopoulos et
383 al., 2015) diminish the mixing in this region, leading to rapid shoaling of the mixed layer. The number of
384 eddies has a minor peak at approximately 15° N. This region has a predominance of anticyclonic eddies
385 (Zhan et al., 2014). The impact of the dominant anticyclonic eddies is visible in the MLD climatology,
386 with deeper mixed layers at approximately 15° N (Fig. 3 and 8). The above results indicate that the
387 frequent eddies in the Red Sea significantly impact the MLD variability by enhancing/diminishing the
388 mixing.

389 **3.4 Influence of Tokar gap winds during the summer**

390 The Tokar gap is one of the largest gaps in the high orography located on the African coast of the Red
391 Sea, near 19° N. Strong winds are funneled to the Red Sea through this gap which last for few days to
392 weeks. Figure 8a shows the u-component of CFSR hourly surface wind at the Tokar region from 1996 to
393 2006. From the figure, it shows that the strong wind events occur during summer every year while the
394 intensity and duration of the event varies from year to year. Tokar gap winds frequently attain a speed of
395 15 m s⁻¹. Previous research also show similar results (Jiang et al., 2009; Ralston et al., 2013; Zhai and
396 Bower, 2013). Zhai and Bower (2013) reported that wind speed may reach 20 to 25m s⁻¹ based on ship-

397 based observations. Figure 8b show that the onset of 2001 Tokar event was on 20th July and continued till
398 20th August, where the maximum wind speed occurred during this period compared to rest of the year.
399 These strong winds generate strong turbulence in the surface water, which enhances vertical mixing.



400

401 **Figure 9.** U-component of the [CFSR](#) hourly surface wind near the Tokar region (38.5° E, 18.5° N) a)
402 from year 1996 to 2006 and b) for the year 2001. The ellipse indicates the TG event in the year 2001.

403 The temperature and salinity profiles measured during summer 2001 (13-14 Aug 2001), which coincided
404 with the Tokar event are shown in [Fig. 10a-b](#) (Sofianos and Johns, 2007; Zhai and Bower, 2013). The
405 signature of Tokar event is clearly visible in the satellite-derived SLA, with well-defined cyclonic and

Deleted: (

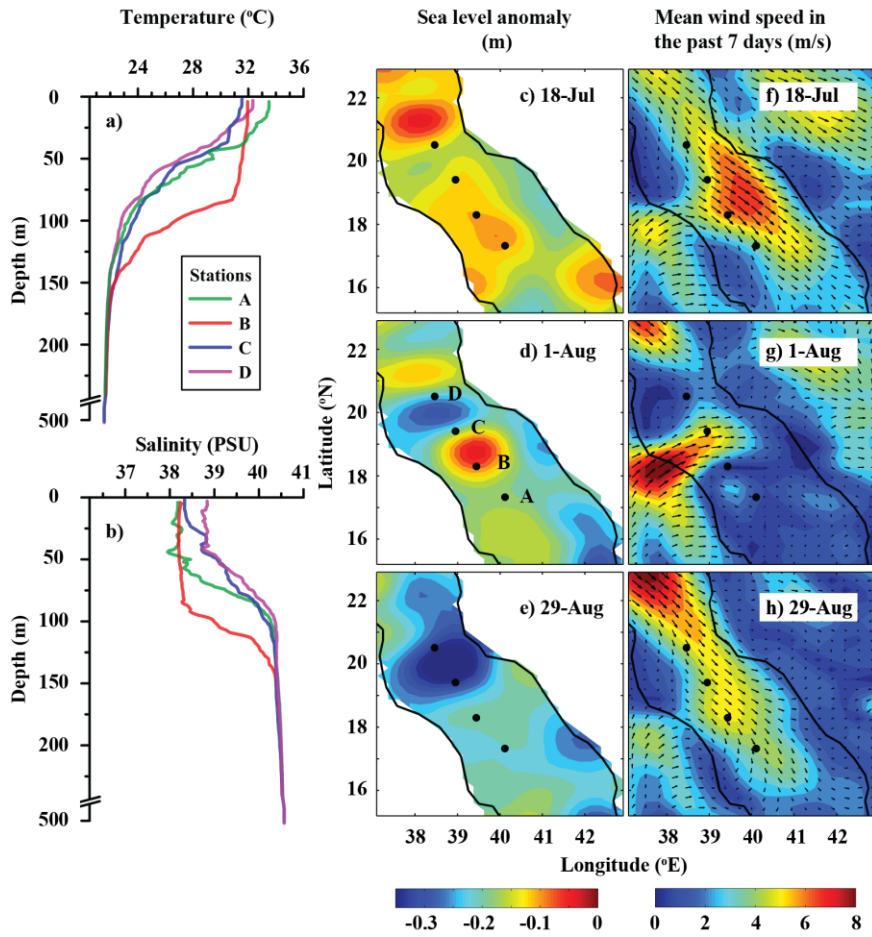
Deleted: (

Deleted:)

409 anticyclonic eddies to the north and south of the Tokar gap respectively (Fig. 10c-e). Both eddies have
410 basin-wide influence and radii between 70-80 km. Corresponding wind speed pattern (averaged for the
411 previous 7 days) is shown (Fig. 10f-h). The profiles to the north and south of the jet axis display a
412 significant difference in MLD, with a deeper mixed layer in the south. Station A is far from both cyclonic
413 and anticyclonic eddies and shows the expected MLD during this period. The presence of the anticyclonic
414 eddy at station B enhances strong downwelling, extending the mixing to a depth of approximately 80 m.
415 It is to be noted that the entire Red Sea basin is well stratified during this period, with MLDs ranging
416 from 10 m to 15 m. Stations C and D are located at the edge of the cyclonic eddy, and both have shallower
417 thermocline and mixed layer.

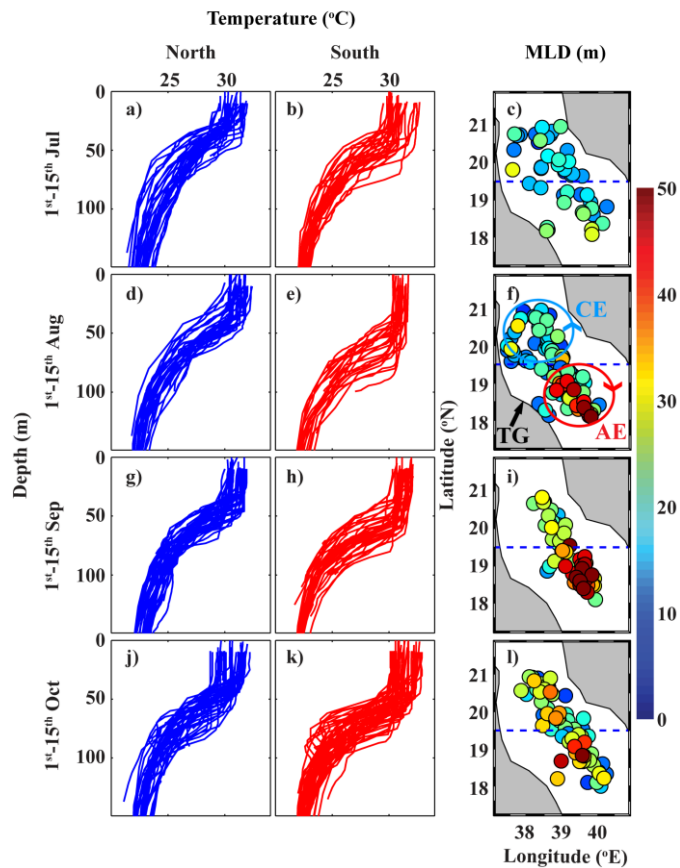
Deleted:

Deleted: s



421 **Figure 10.** (a) The CTD measured temperature and salinity profiles during 13-14 Aug 2001. (b) SLA
 422 maps and (c) wind speed and direction (averaged for the previous one week) in the Tokar region, before,
 423 during and after the Tokar event. [The temperature and salinity profiles are received through personal](#)
 424 [communication from](#) (Sofianos and Johns, 2007).

425 The MLDs of all the available profiles in the Tokar region before, during, just after and after a month of
426 the Tokar event are plotted in [Fig. 11](#) (profiles for the first 15 days of each month are displayed). The
427 mean MLD, standard deviation and number of profiles are given in Table 1. Before the Tokar event, the
428 southern and northern sides of the Tokar axis (18° N- 19.5° N and 19.5° N- 21° N, respectively) displayed
429 similar mixed layers ([Fig. 11a-c](#)). During the Tokar event, the southern side experienced enhanced
430 mixing, while the northern side show shallow mixed layer ([Fig. 11d-f](#)).



431

432 **Figure 11.** Temperature profiles from the north of the Tokar axis (left panel, blue curves), south of the
 433 Tokar axis (middle panel, red curves) and the corresponding MLD (right panel) during the first 15 days
 434 of each month from July to October. The dashed line passes through 19.5° N, roughly separating the north
 435 and south of the Tokar axis. MLD of each profile is represented by the filled colors. The blue and red
 436 circles in (f) schematically represent cyclonic and anticyclonic eddies during Tokar event, respectively.

437 **Table 1.** The mean MLD in the north and south of Tokar jet axis from July to October.

1-15 th days of the Month	Mean		Standard deviation		Number of profiles	
	North	South	north	south	north	south
Jul (before)	20	26	5	8	19	12
Aug (during)	24	38	8	17	27	24
Sep (just after)	30	52	11	14	27	27
Oct (after one month)	31	34	9	12	36	30

438 The anticyclonic part of the Tokar induced eddies enhances downwelling and the associated deepening
 439 of the mixed layer along the southern side of the jet axis, while the cyclonic eddies generate upwelling
 440 and the associated shoaling of the mixed layer along the northern side. The profiles in September (just
 441 after the Tokar event) show the southern side is well mixed by the event, which leads to an average
 442 difference of 20 m in the MLDs between both sides of the Tokar axis (Fig. 11g-i). The signature of the
 443 Tokar events in the MLDs (MLD difference between north and south of the jet axis) has disappeared by
 444 October (one month after the Tokar event, Fig. 11j-l).

445 The mixing in the Tokar region during summer is the sum of the two mechanisms, the wind-induced
 446 turbulent mixing and the secondary circulation (eddies) induced by the wind. Both mechanisms act in the
 447 same direction in the southern side of the jet axis resulting in enhanced mixing, while they act in opposite

Deleted:

449 direction in the northern side leading to reduced mixing. Further studies are required for proper
450 quantification of the contribution of each mechanism. In summary, [during the summer](#), the turbulence
451 induced by strong wind and [the impact of anticyclonic eddy](#) enhance vertical mixing [in the southern side](#)
452 [of jet axis, while the wind-induced mixing is diminished by the presence of cyclonic eddy in the northern](#)
453 [side of the jet axis](#).

454 4 Conclusions

455 A detailed information on MLD variability is crucial for understanding the physical and biological
456 processes in the ocean. The goals of this study were to produce a climatology record of MLD for the Red
457 Sea and to investigate the role of major forces on MLD changes. With the help of in situ temperature
458 profiles from CTD, XBT, MBT and profiler float measurements, the MLD variability in the Red Sea has
459 been explored for the first time and the MLD climatology is produced for every 0.5 degrees along the
460 main axis. [The climatology](#) reasonably captured all the major features [of MLD variability in the Red Sea](#).
461 The present work provides a [climatological mean](#) of the MLD structure in the Red Sea and its seasonal
462 variability. Influences of wind stress, heat flux, evaporation and precipitation are explored. Further, the
463 impact of the Tokar gap jet stream winds, [the](#) eddies and the upwelling events in the northern Red Sea are
464 investigated.

465 A deep ventilation process associated with the winter cooling is observed across the entire Red Sea during
466 the months of December to February ([Fig. 3](#)). Similarly, very shallow MLDs [associated with increased](#)
467 [short-wave radiation](#) are detected all along the region from May to Jun. The climatological winter MLD
468 ranges from ~40 to 85 m (in January). Similarly, the climatological summer MLD varies from 10 to ~20
469 m (in June), which may reach to >40 (in July). The mixed layer becomes deeper toward the north, even
470 though the pattern is not linear [with increasing latitude](#). The largest amplitude of variability is observed
471 at the tip of the northern Red [Sea which](#) is associated with strong deep convection during the winter and
472 shoaling during the summer. The region at approximately 19° N experienced deeper [MLD than typical of](#)
473 [elsewhere in the Red Sea](#). [This region experienced enhanced mixing during winter by surface cooling,](#)
474 [and during summer by both the Tokar gap wind induced turbulent mixing and the formation of the](#)

Deleted: s

Deleted: associated

Deleted: ies

Deleted:

Deleted: impact

Deleted: ¶

Deleted: Averaging the MLDs can result in slightly lower values, but

Deleted: t

Deleted: climatology

Deleted: general picture

Deleted: also

Deleted: strong stratification

Deleted: Sea, and

Deleted: than average MLD for most of the year

490 [anticyclonic eddy](#). The deepest mixed layer is observed at the northern tip of Red Sea during the winter,
491 but the deep nature of northern mixed layer is almost limited to the winter months.

Deleted: This region experienced enhanced mixing during winter by surface cooling during winter, and during summer by the Tokar gap wind induced turbulent mixing and the formation of anticyclonic eddy during summer.

492 Correlation analyses between MLD and forcing factors displayed the influence of major forces on MLD,
493 from north to south of the Red Sea. In general, the wind stress mainly controls the MLD variability in the
494 southern part of the Red Sea, heat flux and evaporation dominate in the central region, and all the three
495 forces contribute in the northern region. Coinciding drops are observed in the correlations for all the
496 selected forcing factors around the previously reported main eddy locations. In these locations, eddies
497 override the controls of the other main forces, namely, wind stress, heat flux and fresh-water flux. The
498 quasi-permanent cyclonic gyre and upwelling in the northern Red Sea lead to the shoaling of the mixed
499 layer at $\sim 26.5^\circ$ N throughout almost the whole year.

500 [The anticyclonic eddy induced by Tokar gap winds, and the wind induced turbulent mixing together](#)
501 [enhanced the deep convection and mixing along the southern side of the Tokar jet axis during the summer,](#)
502 [while the wind induced mixing is reduced by the cyclonic eddy.](#) This leads to a deepening of the mixed
503 layer, to >40 m, while the MLDs in the rest of the Red Sea are <20 m. The effect of Tokar event is seen
504 in the profiles of late July to early [August which](#) gradually disappeared by October. The frequent eddies,
505 associated with surface circulation and Tokar events, have [a](#) strong impact on the MLD structure of the
506 Red Sea.

Deleted: The Tokar gap winds during the summer enhanced the deep convection and mixing along the southern side of the Tokar jet axis.

Deleted: August, and

Deleted: is

507 **Data availability**

508 The climatology data produced in this manuscript is available from the repository "Figshare"
509 (DOI:10.6084/m9.figshare.5539852). The monthly mean values of heat fluxes and wind stress data are
510 available from Tropflux (http://www.incois.gov.in/tropflux_datasets/data/monthly/). [The monthly mean](#)
511 [values of evaporation are accessible from](#) OAflux
512 (ftp://ftp.whoi.edu/pub/science/oaflux/data_v3/monthly/evaporation/). The precipitation data is available
513 from TRMM (<https://pmm.nasa.gov/data-access/downloads/trmm>).

Deleted: The monthly mean values of evaporation is available from

524 **Acknowledgments**

525 This project was funded by the Deanship of Scientific Research (DSR), King Abdulaziz University, under
526 grant number (438/150/129). The authors, therefore, acknowledge the DSR's technical and financial
527 support. The authors acknowledge TropFlux, OAFlux, TRMM, AVISO, CFSR, World Ocean Database
528 and Coriolis data center for making their data products publicly available. The authors also [acknowledge](#)
529 the institutes who have provided CTD profiles from different cruises. The author CPA acknowledges the
530 Deanship of Graduate Studies, King Abdulaziz University, Jeddah, for providing a Ph.D. Fellowship.

Deleted: acknowledges

531 **References**

532 Abdulla, C. P., Alsaafani, M. A., Alraddadi, T. M. and Albarakati, A. M.: Estimation of Mixed Layer
533 Depth in the Gulf of Aden: A New Approach, PLoS One, 11(10), e0165136,
534 doi:10.1371/journal.pone.0165136, 2016.

535 Aboobacker, V. M., Shanas, P. R., Alsaafani, M. A. and Albarakati, A. M.: Wave energy resource
536 assessment for Red Sea, Renew. Energy, 1–13, doi:10.1016/j.renene.2016.09.073, 2016.

537 Albarakati, A. M. and Ahmad, F.: Variation of the surface buoyancy flux in the Red Sea, Indian J. Mar.
538 Sci., 42(6), 717–721, 2013.

539 Alsaafani, M. A. and Shenoï, S. S. C.: Seasonal cycle of hydrography in the Bab el Mandab region,
540 southern Red Sea, J. Earth Syst. Sci., 113(3), 269–280, doi:10.1007/BF02716725, 2004.

541 Alsaafani, M. A. and Shenoï, S. S. C.: Water masses in the Gulf of Aden, J. Oceanogr., 63(1), 1–14,
542 doi:10.1007/s10872-007-0001-1, 2007.

543 Beal, L. M., Field, A. and Gordon, A. L.: Spreading of Red Sea overflow waters in the Indian Ocean, J.
544 Geophys. Res., 105(C4), 8549–8564, doi:10.1029/1999JC900306, 2000.

546 Bower, A. S. and Farrar, J. T.: Air-sea interaction and horizontal circulation in the Red Sea, in *The Red*
547 *Sea*, pp. 329–342, Springer., 2015.

548 Boyer, T. P. and Levitus, S.: Quality control and processing of historical temperature, salinity, and
549 oxygen data, NOAA Tech. Rep., NESDIS 81, 65, 1994.

550 de Boyer Montegut, C., Madec, G., Fischer, A. S., Lazar, A. and Iudicone, D.: Mixed layer depth over
551 the global ocean: An examination of profile data and a profile-based climatology, *J. Geophys. Res. C*
552 *Ocean.*, 109(12), 1–20, doi:10.1029/2004JC002378, 2004.

553 Carlson, D. F., Fredj, E. and Gildor, H.: The annual cycle of vertical mixing and restratification in the
554 Northern Gulf of Eilat/Aqaba (Red Sea) based on high temporal and vertical resolution observations,
555 *Deep. Res. Part I Oceanogr. Res. Pap.*, 84, 1–17, doi:10.1016/j.dsr.2013.10.004, 2014.

556 Chelton, D. B., Schlax, M. G., Freilich, M. H. and Milliff, R. F.: Satellite measurements reveal
557 persistent small-scale features in ocean winds, *Science* (80-.), 303(5660), 978–983, 2004.

558 Chelton, D. B., Schlax, M. G. and Samelson, R. M.: Global observations of nonlinear mesoscale eddies,
559 *Prog. Oceanogr.*, 91(2), 167–216, doi:10.1016/j.pocean.2011.01.002, 2011.

560 Chen, D., Busalacchi, A. J. and Rothstein, L. M.: The roles of vertical mixing, solar radiation, and wind
561 stress in a model simulation of the sea surface temperature seasonal cycle in the tropical Pacific Ocean,
562 *J. Geophys. Res.*, 99(C10), 20345, doi:10.1029/94JC01621, 1994.

563 Cheng, L., Zhu, J., Cowley, R., Boyer, T. P. and Wijffels, S.: Time, probe type, and temperature
564 variable bias corrections to historical expendable bathythermograph observations, *J. Atmos. Ocean.*
565 *Technol.*, 31(8), 1793–1825, doi:10.1175/JTECH-D-13-00197.1, 2014.

566 Clifford, M., Horton, C., Schmitz, J. and Kantha, L. H.: An oceanographic nowcast/forecast system for

567 the Red Sea, *J. Geophys. Res. Ocean.*, 102(C11), 25101–25122, doi:10.1029/97JC01919, 1997.

568 D’Ortenzio, F., Iudicone, D., de Boyer Montegut, C., Testor, P., Antoine, D., Marullo, S., Santoleri, R.
569 and Madec, G.: Seasonal variability of the mixed layer depth in the Mediterranean Sea as derived from
570 in situ profiles, *Geophys. Res. Lett.*, 32(12), L12605, doi:10.1029/2005GL022463, 2005.

571 Dewar, W. K.: Mixed layers in Gulf Stream rings, *Dyn. Atmos. Ocean.*, 10(1), 1–29, 1986.

572 Ducet, N., LaTraon, P. Y. and Reverdin, G.: Global high-resolution mapping of ocean circulation from
573 TOPEX/Poseidon and ERS-1 and -2, *J. Geophys. Res. Ocean.*, 105(C8), 19477–19498,
574 doi:10.1029/2000JC900063, 2000.

575 Fox-Kemper, B., Ferrari, R. and Hallberg, R.: Parameterization of Mixed Layer Eddies. Part I: Theory
576 and Diagnosis, *J. Phys. Oceanogr.*, 38(6), 1145–1165, doi:10.1175/2007JPO3792.1, 2008.

577 Hausmann, U., McGillicuddy, D. J. and Marshall, J.: Observed mesoscale eddy signatures in Southern
578 Ocean surface mixed-layer depth, *J. Geophys. Res. Ocean.*, 122(1), 617–635,
579 doi:10.1002/2016JC012225, 2017.

580 Jiang, H., Farrar, J. T., Beardsley, R. C., Chen, R. and Chen, C.: Zonal surface wind jets across the Red
581 Sea due to mountain gap forcing along both sides of the Red Sea, *Geophys. Res. Lett.*, 36(19), 1–6,
582 doi:10.1029/2009GL040008, 2009.

583 Johns, W. E., Jacobs, G. A., Kindle, J. C., Murray, S. P. and Carron, M.: Arabian marginal seas and
584 gulfs. University of Miami RSMAS Technical Report., University of Miami, Florida, USA., 1999.

585 Kara, A. B., Rochford, P. A. and Hurlburt, H. E.: Mixed layer depth variability over the global ocean, *J.*
586 *Geophys. Res.*, 108(C3), 3079, doi:10.1029/2000JC000736, 2003.

587 Keerthi, M. G., Dyn, C., Monte, C. D. B., Lengaigne, M., Vialard, J., Boyer Montégut, C.,
588 Muraleedharan, P. M., Dyn, C., Monte, C. D. B., Keerthi, M. G., Lengaigne, M., Vialard, J., Boyer
589 Montégut, C., Muraleedharan, P. M., de Boyer Montégut, C. and Muraleedharan, P. M.: Interannual
590 variability of the Tropical Indian Ocean mixed layer depth, *Clim. Dyn.*, 40(3–4), 743–759,
591 doi:10.1007/s00382-012-1295-2, 2012.

592 Keerthi, M. G., Lengaigne, M., Drushka, K., Vialard, J., Montegut, C. D. B., Pous, S., Levy, M. and
593 Muraleedharan, P. M.: Intraseasonal variability of mixed layer depth in the tropical Indian Ocean, *Clim.*
594 *Dyn.*, 46(7–8), 2633–2655, doi:10.1007/s00382-015-2721-z, 2016.

595 LaTraon, P. Y. and Dibarboure, G.: Mesoscale Mapping Capabilities of Multiple-Satellite Altimeter
596 Missions, *J. Atmos. Ocean. Technol.*, 16(9), 1208–1223, doi:10.1175/1520-
597 0426(1999)016<1208:MMCOMS>2.0.CO;2, 1999.

598 Lorbacher, K., Dommenges, D., Niiler, P. P. and Köhl, A.: Ocean mixed layer depth: A subsurface
599 proxy of ocean-atmosphere variability, *J. Geophys. Res. Ocean.*, 111(7), 1–22,
600 doi:10.1029/2003JC002157, 2006.

601 Papadopoulos, V. P., Zhan, P., Sofianos, S. S., Raitso, D. E., Qurban, M., Abualnaja, Y., Bower, A. S.,
602 Kontoyiannis, H., Pavlidou, A., Asharaf, T. T. M., Zarokanellos, N. and Hoteit, I.: Factors governing
603 the deep ventilation of the Red Sea, *J. Geophys. Res. Ocean.*, 120(11), 7493–7505,
604 doi:10.1002/2015JC010996, 2015.

605 Polovina, J., Mitchum, G. T. and Evans, T.: Decadal and basin-scale variation in mixed layer depth and
606 the impact on biological production in the Central and North Pacific , 1960-88, *Deep Sea Res.*, 42(10),
607 1701–1716, 1995.

608 Praveen Kumar, B., Vialard, J., Lengaigne, M., Murty, V. S. N. and McPhaden, M. J.: TropFlux: air-sea
609 fluxes for the global tropical oceans—description and evaluation, *Clim. Dyn.*, 38(7–8), 1521–1543,

610 doi:10.1007/s00382-011-1115-0, 2012.

611 Praveen Kumar, B., Vialard, J., Lengaigne, M., Murty, V. S. N., McPhaden, M. J., Cronin, M. F.,
612 Pinsard, F. and Gopala Reddy, K.: TropFlux wind stresses over the tropical oceans: evaluation and
613 comparison with other products, *Clim. Dyn.*, 40(7–8), 2049–2071, doi:10.1007/s00382-012-1455-4,
614 2013.

615 Quadfasel, D. and Baudner, H.: Gyre-scale circulation cells in the red-sea, *Oceanol. Acta*, 16(3), 221–
616 229, 1993.

617 Ralston, D. K., Jiang, H. and Farrar, J. T.: Waves in the Red Sea: Response to monsoonal and mountain
618 gap winds, *Cont. Shelf Res.*, 65, 1–13, doi:10.1016/j.csr.2013.05.017, 2013.

619 Smith, K. S. and Marshall, J.: Evidence for Enhanced Eddy Mixing at Middepth in the Southern Ocean,
620 *J. Phys. Oceanogr.*, 39(1), 50–69, doi:10.1175/2008JPO3880.1, 2009.

621 Sofianos, S. S. and Johns, W. E.: An Oceanic General Circulation Model (OGCM) investigation of the
622 Red Sea circulation, 1. Exchange between the Red Sea and the Indian Ocean, *J. Geophys. Res.*,
623 107(C11), 3196, doi:10.1029/2001JC001184, 2002.

624 Sofianos, S. S. and Johns, W. E.: Observations of the summer Red Sea circulation, *J. Geophys. Res.*
625 *Ocean.*, 112(6), 1–20, doi:10.1029/2006JC003886, 2007.

626 Sofianos, S. S., Johns, W. E. and Murray, S. P.: Heat and freshwater budgets in the Red Sea from direct
627 observations at Bab el Mandeb, *Deep. Res. Part II Top. Stud. Oceanogr.*, 49(7–8), 1323–1340,
628 doi:10.1016/S0967-0645(01)00164-3, 2002.

629 Sutton, P. J., Worcester, P. F., Masters, G., Cornuelle, B. D. and Lynch, J. F.: Ocean mixed layers and
630 acoustic pulse propagation in the Greenland Sea, *J Acoust Soc Am*, 94(3), 1517–1526,

631 doi:10.1121/1.408130, 2014.

632 Tragou, E., Garrett, C., Outerbridge, R. and Gilman, C.: The Heat and Freshwater Budgets of the Red
633 Sea, *J. Phys. Oceanogr.*, 29(10), 2504–2522, doi:10.1175/1520-
634 0485(1999)029<2504:THAFBO>2.0.CO;2, 1999.

635 Turner, J. S.: *Buoyancy effects in fluids*, Cambridge University Press, Cambridge., 1973.

636 Yao, F., Hoteit, I., Pratt, L. J., Bower, A. S., Zhai, P., Köhl, A. and Gopalakrishnan, G.: Seasonal
637 overturning circulation in the Red Sea: 1. Model validation and summer circulation, *J. Geophys. Res.*
638 *Ocean.*, 119(4), 2238–2262, doi:10.1002/2013JC009004, 2014a.

639 Yao, F., Hoteit, I., Pratt, L. J., Bower, A. S., Köhl, A., Gopalakrishnan, G. and Rivas, D.: Seasonal
640 overturning circulation in the Red Sea: 2. Winter circulation, *J. Geophys. Res. Ocean.*, 119(4), 2263–
641 2289, doi:10.1002/2013JC009331, 2014b.

642 Zeng, L. and Wang, D.: Seasonal variations in the barrier layer in the South China Sea: characteristics,
643 mechanisms and impact of warming, *Clim. Dyn.*, 48(5–6), 1911–1930, doi:10.1007/s00382-016-3182-
644 8, 2017.

645 Zhai, P. and Bower, A. S.: The response of the Red Sea to a strong wind jet near the Tokar Gap in
646 summer, *J. Geophys. Res. Ocean.*, 118(1), 422–434, doi:10.1029/2012JC008444, 2013.

647 Zhan, P., Subramanian, A. C., Yao, F. and Hoteit, I.: Eddies in the Red Sea: A statistical and dynamical
648 study, *J. Geophys. Res. Ocean.*, 119(6), 3909–3925, doi:10.1002/2013JC009563, 2014.

649

Marked-up supplementary file

1 Supporting Information for

2 **Mixed layer depth variability in the Red Sea**

3 Cheriyei P. Abdulla^{1*}, Mohammed A. Alsaafani^{1,2}, Turki M. Alraddadi¹, and Alaa M. Albarakati¹

4 ¹Department of Marine Physics, Faculty of Marine Sciences, King Abdulaziz University, Jeddah, Saudi Arabia.

5 ²Department of Earth & Environmental Sciences, Faculty of Science, Sana'a University, Yemen.

6
7 *Correspondence to:* Cheriyei P. Abdulla (acp@stu.kau.edu.sa)

8

9

10 **Contents of this file**

11 [1. Figure S1](#)

12 [2. Figure S2](#)

13 [3. Figure S3](#)

14 [4. Figure S4](#)

15

16

17

Deleted: <#>Figure S1¶
<#>Tables S1¶
<#>Tables S2¶
<#>Tables S3¶
<#>Tables S4¶

23 **Introduction**

24 The figures and tables which support the results discussed in the manuscript “**Mixed layer depth**
25 **variability in the Red Sea**” are given below. Detailed description on the attached figures and tables is
26 given in the manuscript. A brief summary is given in the following lines.

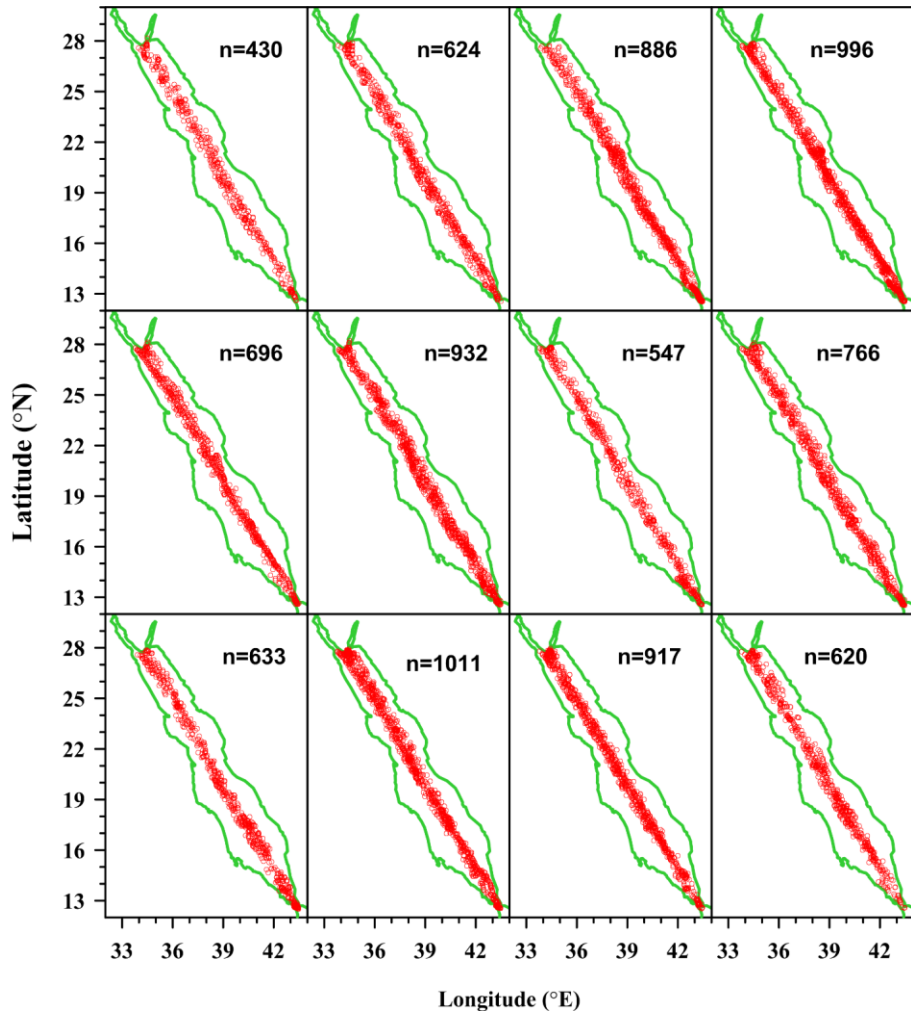
27 Figure S1 shows the monthly distribution of the temperature profiles along the main-axis of Red Sea. The
28 number of profiles are marked at the top right corner in each sub-figure. This document also includes bar
29 charts showing the number of selected profiles along the main-axis of Red Sea based on the year (Fig.
30 S2) and month (Fig. S3) of measurement. Similarly, a bar chart is included to show the number of profiles
31 with salinity values in the study area (Fig. S4).

Deleted: Figure S1 shows the monthly distribution of the temperature profiles along the main-axis of Red Sea. The number of profiles are marked at the top right corner in each sub-figure. This document also includes tables of number of profiles removed at different steps of quality checking procedure and the number of selected profiles along the main-axis of Red Sea based on the month and year of measurement. Similarly, a table is included to show the number of profiles with salinity values in the study area. ¶

32

33

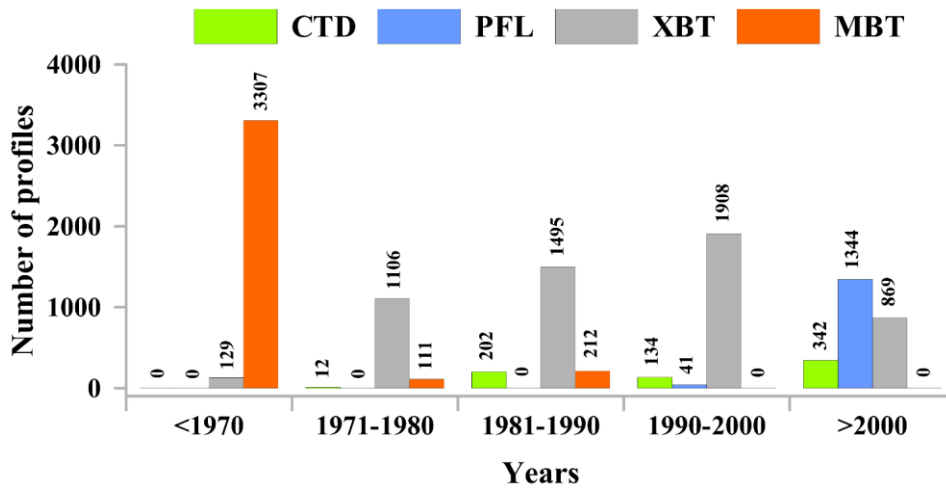
34



45 **Figure S1.** Monthly distribution of the temperature profiles along the main-axis of Red Sea. The number
46 of profiles is marked at the top right corner. The different steps of quality control are discussed in the
47 main manuscript.

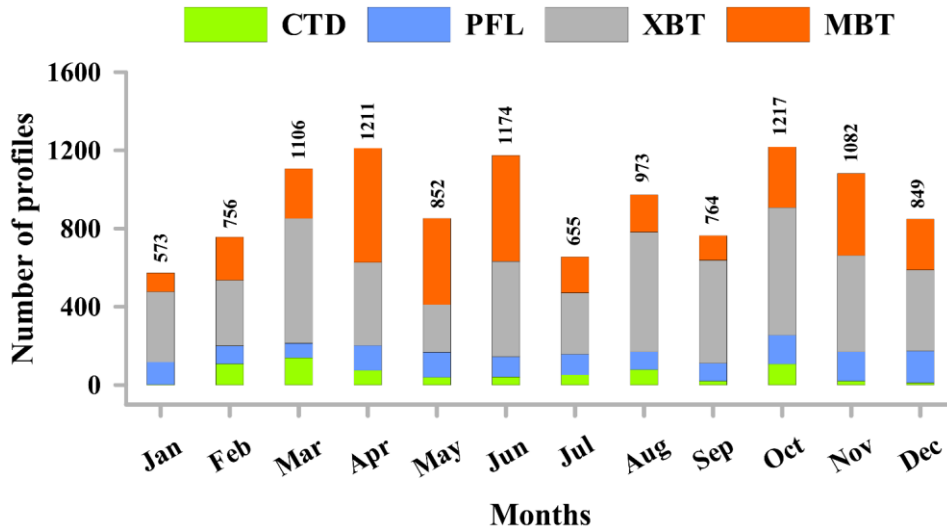
Deleted: are

Deleted: r



52
53
54 **Figure S2.** Number of temperature profiles along the main-axis of Red Sea based on the year of
55 measurement.

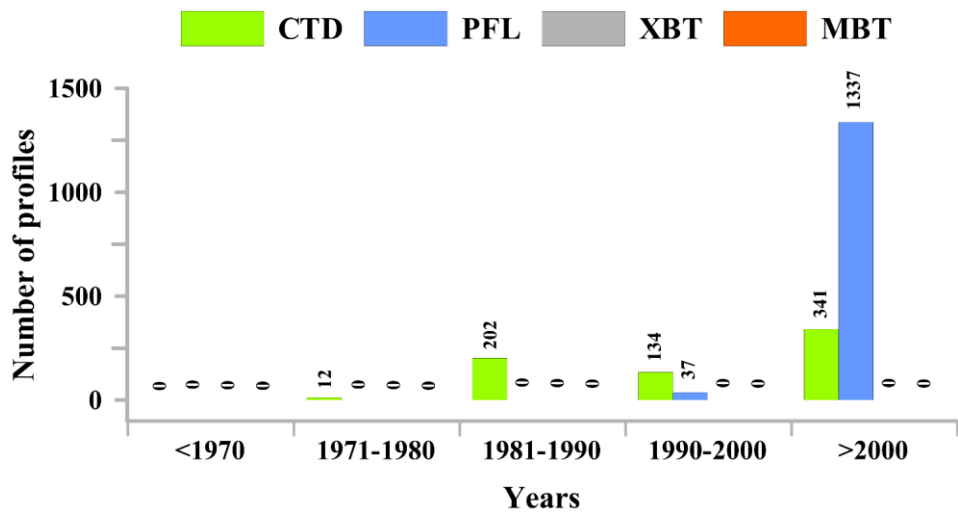
56
57
58



61
62

63 **Figure S3.** Number of temperature profiles along the main-axis of Red Sea based on the month of
64 measurement.

65
66
67
68
69



71 **Figure S4.** Number of total salinity profiles available in the entire Red Sea based on the year of
 72 measurement.